JCTC Journal of Chemical Theory and Computation

Article

pubs.acs.org/JCTC

Solvent Effects on Electronically Excited States Using the Conductor-Like Screening Model and the Second-Order Correlated Method ADC(2)

Bernd Lunkenheimer and Andreas Köhn*

Institut für Physikalische Chemie, Johannes Gutenberg-Universität, 55099 Mainz, Germany

Supporting Information

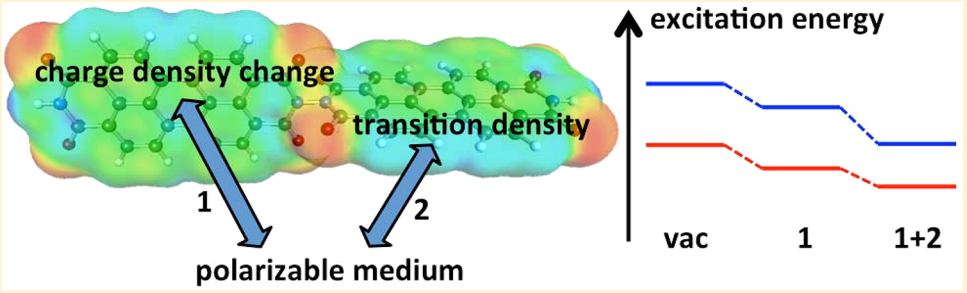

ABSTRACT: The conductor-like screening model (COSMO) is used to treat solvent effects on excited states within a correlated method based on the algebraic-diagrammatic construction through second-order ADC(2). The origin of solvent effects is revisited, and it is pointed out that two types of contributions have to be considered. One effect is due to the change of the solute's charge distribution after excitation, which triggers a reorganization of the solvent. Initially, only the electronic degrees of freedom adapt to the new charge distribution (nonequilibrium case); for sufficiently long-lived states, the reorientation of the solvent molecules contributes, as well (equilibrium case). The second effect is the coupling of the transition densities to the fast (purely electronic) response of the solvent molecules, which can be viewed as excitonic coupling between solute and solvent molecules. This interaction is also responsible for the screening of excitonic couplings between spatially separated chromophores. While most previous implementations of comparable continuum solvation models only include either of both effects, we argue that both contributions should be taken into account. Both effects can significantly influence the excitation energy and excited state properties of the solute, as exemplified for the $\pi-\pi^*$ and $n-\pi^*$ excitations of acrolein, and no a priori reason exists to neglect either. The implementation is also tested for the excitonic coupling of the ethene dimer where linear response contributions are indispensable for recovering the screening effects due to the solvent. Example applications to larger cases are provided, too. We discuss the excitonic coupling in a linked dyad consisting of two perylene-tetracarboxy-diimide chromophores, and the solvent effects on an intramolecular charge-transfer state of 4-(*N*,*N*-dimethylamino)benzonitrile.

1. INTRODUCTION

The majority of present day research in chemistry and molecular physics focuses on condensed phase systems. In many cases, these systems still consist of distinct molecules, and hence, theoretical predictions about the properties of the system can be made on the basis of quantum-chemical calculations for the individual constituents. The properties of an isolated molecule, however, may differ strongly from those of a molecule embedded in a condensed phase system, and interactions with the surrounding molecules must be taken into account in some way. In the absence of translational symmetry, the explicit quantum chemical treatment of the entire system is computationally too demanding in most cases. A promising approach to proceed into this direction is a partitioning into coupled subsystems.[1] A frequently used approximation couples the quantum-mechanical treatment of a small kernel system and a classical molecular-mechanics treatment of the remainder (QM/MM-schemes).[2−8] While this scheme keeps a maximum of the atomistic picture of the interactions, the necessary statistical averaging can still be rather involved and difficult to converge. For strongly fluctuating environments with low order (in particular the case of a molecule in a solvent), the statistical average over the surrounding molecules can be approximated by a polarizable continuum with a characteristic dielectric constant ε. This is the basic idea of the continuum solvation models (CSMs).[9−13] The most widely used variants are known under the acronyms PCM (polarizable continuum model)[14] and COSMO (conductor-like screening model).[15] While these models are certainly best suited for the description of molecules in solvents, they may also be used as a simple means to estimate the effect of a polarizable environment in case of more ordered systems.

Received: September 3, 2012
Published: December 4, 2012

In this contribution, we will use the COSMO approach to describe environment effects on excited electronic states. Simple solvation models for the treatment of dye molecules in solution, mostly employing spherical cavities, date back to early works in the 1950s, e.g. that of McRae,[16] based on models of Kirkwood[17] and Onsager.[18] In connection with ab initio quantum chemistry, early applications were based on the Kirkwood model, for example the MCSCF implementations of Mikkelsen and co-workers,[19−21] later applied to coupled-cluster wave functions,[22] too. Implementations within the PCM framework have been reported for, e.g., time-dependent Hartree−Fock (TDHF),[23] multiconfigurational self-consistent-field (MCSCF),[24] configuration interaction with single replacements (CIS),[25] time-dependent density functional theory (TDDFT),[26] and multireference configuration interaction (MRCI).[27] More recently, PCM was also applied to coupled-cluster (CC) theory[28−30] and symmetry-adapted cluster configuration interaction (SAC-CI).[31] For COSMO, so far only the application to MRCI[32] has been reported.

Here, we combine COSMO and the ADC(2) method (algebraic diagrammatic construction through second-order),[33] a method that is very closely related[34] to the second-order approximate coupled-cluster (CC2) method.[35] These methods have proven to be very successful in the application to molecular excited states, typically for organic compounds,[34,36] in particular in cases where usual density functionals tend to fail, as for charge-transfer states[37,38] or T_1 states of triplet-instable systems.[39] Comparatively large systems are accessible due to a very efficient implementation[34] which uses the resolution-of-the-identity trick[40] (also known as density-fitting). The present implementation is based on the RICC2 module.[41] of the TURBOMOLE program package.[42] The application of solvation models to correlated methods is by no means trivial, basically owing to the nonlinear nature of the underlying effective Schrödinger equation. We will investigate the two different approaches to derive solvent-dependent terms, the state-specific approach and the linear-response approach, in particular in the light of describing the screening of excitonic coupling effects in multichromophoric compounds.

We will outline the basic theory in section 2 and specifically report on the application of COSMO to CIS and ADC(2) in section 3. In section 4, finally, we will present sample calculations which serve to discuss some features of the model and to show the possible range of application of the present implementation.

2. CONTINUUM SOLVATION MODELS: THEORY AND NOTATION

This section is intended as a quick review of continuum solvation models (CSMs). We will focus on apparent surface charge methods, a category into which the two most popular variants fall, PCM and COSMO. Basically all equations given below apply to both models. Most of the exited state formalism is a review of previous work, but we will give a different perspective of the two versions, the linear response approach and the state-specific approach, which in the literature are viewed as alternatives.[43,44] We will argue that these approaches describe complementary effects and that terms from both approaches should be used together in a combined approach. We note that a similar discussion exists in the context of polarizable force-field embedding approaches.[45] While the terms motivated by the state-specific approach serve to describe the effect of a change in the charge distribution due to the electronic transition, the terms from the response approach add the effect of electronic excitation energy transfer coupling (in the following we will prefer the shorter term *excitonic coupling*) to surrounding solvent molecules. The response terms are also responsible for the screening of excitonic couplings between excitations on different parts of the molecule. Finally, this section serves as an introduction to our notation, which mainly follows that used by Cammi and co-workers, see, e.g., ref 43.

2.1. Free Energy of the Solute's Electronic States. All CSMs have in common that the statistical average over solvent molecules is replaced by a polarizable continuum. The solute is placed in a cavity within the continuum. The electric potential of the molecule causes a polarization of the surrounding medium (also called reaction field), and the resulting electrostatic interactions are used to estimate the free energy of solvation. Apparent surface charge methods, like PCM and COSMO, represent the induced polarization by charges spread out on the cavity surface.

Following the notation of Cammi and co-workers,[43] we will denote with $V(s)$ the potential induced on the cavity surface S (and $s \in S$ is a surface coordinate). The response of the solvent gives rise to an apparent surface charge $Q(s)$, which can be expressed as

$$Q(s) = -\int_S \mathrm{d}s'\, A^{-1}(s, s')V(s') \tag{1}$$

The response kernel A differs for the various CSMs; for an overview, see, e.g., ref 10.

Introducing the operator measuring the solute potential on the cavity surface, $\hat{V}(s)$, and the operator measuring the surface charge $\hat{Q}(s)$, the effective solvation potential of a solute with wave function $|\Psi_I\rangle$ takes the form

$$\hat{\mathcal{V}}[|\Psi_I\rangle] = \int_S \mathrm{d}s\, \langle\Psi_I|\hat{Q}(s)|\Psi_I\rangle\hat{V}(s) \equiv \langle\Psi_I|\hat{\mathbf{Q}}|\Psi_I\rangle\cdot\hat{\mathbf{V}} \tag{2}$$

where I enumerates the electronic states (typically the ground state $I = 0$ or an energetically low-lying excited state will be of interest). Here, again following the earlier literature,[43] we introduced a vector dot product notation for convenience which either can be interpreted as a shorthand way to write the integral or as a sum over finite elements (which resembles the actual numerical procedure).

$\hat{\mathcal{V}}[|\Psi_I\rangle]$ depends on the wave function $|\Psi_I\rangle$, and we arrive at a nonlinear Schrödinger equation for the solvated molecule

$$\{\hat{H} + \langle\Psi_I|\hat{\mathbf{Q}}|\Psi_I\rangle\cdot\hat{\mathbf{V}}\}|\Psi_I\rangle = E_I|\Psi_I\rangle \tag{3}$$

The actual free energy $\mathcal{G}_I$ of the solute differs from the above eigenvalue E_I by the work for creating the cavity surface charges, $-{}^1/_2\langle\Psi_I|\hat{\mathbf{Q}}|\Psi_I\rangle\cdot\langle\Psi_I|\hat{\mathbf{V}}|\Psi_I\rangle$, and we hence obtain

$$\begin{aligned}\mathcal{G}_I &= \langle\Psi_I|\hat{H} + \frac{1}{2}\langle\Psi_I|\hat{\mathbf{Q}}|\Psi_I\rangle\cdot\hat{\mathbf{V}}|\Psi_I\rangle \\ &= \langle\Psi_I|\hat{H}|\Psi_I\rangle + \frac{1}{2}\langle\Psi_I|\hat{\mathbf{Q}}|\Psi_I\rangle\cdot\langle\Psi_I|\hat{\mathbf{V}}|\Psi_I\rangle\end{aligned} \tag{4}$$

So far we have assumed that solute and solvent are in equilibrium, that is eq 3 is solved self-consistently. We will henceforth indicate this by "(eq)" for the wave function and related quantities. Introducing the short notation $\langle\Psi_{I(\mathrm{eq})}|\hat{\mathbf{Q}}|\Psi_{I(\mathrm{eq})}\rangle = \mathbf{Q}_{I(\mathrm{eq})}$, $\langle\Psi_{I(\mathrm{eq})}|\hat{\mathbf{V}}|\Psi_{I(\mathrm{eq})}\rangle = \mathbf{V}_{I(\mathrm{eq})}$, we can write the free energy of the equilibrated state as

$$\mathcal{G}_{I(\mathrm{eq})} = \langle\Psi_{I(\mathrm{eq})}|\hat{H}|\Psi_{I(\mathrm{eq})}\rangle + \frac{1}{2}\mathbf{Q}_{I(\mathrm{eq})}\cdot\mathbf{V}_{I(\mathrm{eq})} \tag{5}$$

The assumption of equilibration is appropriate for any sufficiently long-lived state, where long-lived means that its lifetime is much longer than the reorganization time of the solvent. Apart from the electronic ground state, this may be, for example, the lowest singlet or triplet excited state of a molecule. Higher excited states or excited states in systems with open-shell ground states often do not meet the requirement of a sufficiently long lifetime.

For short-lived states, or when considering "vertical" transitions with frozen nuclear degrees of freedom, the solvent cannot fully relax. Only the electronic part of the solvent molecules' polarizability will lead to an immediate response, while the nuclear degrees of freedom, in particular the reorientation of the solvent molecules, remain at the equilibrium position for the initially populated state. In the following, the short-lived state will be denoted $|\Psi_J\rangle$ (without the additional index "(eq)" and $J \neq I$) and the initial state (with respect to which the solvent is relaxed) is notated as $|\Psi_{I(\mathrm{eq})}\rangle$, as introduced above.

The response of the solvent can be split into a slow and a fast component, giving rise to two surface charge operators $\hat{Q}(s) = \hat{Q}^s(s) + \hat{Q}^f(s)$. The slow part describes the response of the solvent's nuclear degrees of freedom, and the fast part is the response of solvent's electrons. While the slow part of the reaction field remains equilibrated with the initial state, the fast part is assumed to instantaneously adapt to the short-lived target state $|\Psi_J\rangle$. The nonlinear Schrödinger equation for this problem is

$$\{\hat{H} + (\langle\Psi_{I(\mathrm{eq})}|\hat{\mathbf{Q}}^{s}|\Psi_{I(\mathrm{eq})}\rangle + \langle\Psi_J|\hat{\mathbf{Q}}^{f}|\Psi_J\rangle)\cdot\hat{\mathbf{V}}\}|\Psi_J\rangle = E_J|\Psi_J\rangle \tag{6}$$

and the free energy becomes

$$\begin{aligned}\mathcal{G}_J^{\mathrm{noneq}} &= \langle\Psi_J|\hat{H} + (\langle\Psi_{I(\mathrm{eq})}|\hat{\mathbf{Q}}^{s}|\Psi_{I(\mathrm{eq})}\rangle + \langle\Psi_J|\hat{\mathbf{Q}}^{f}|\Psi_J\rangle)\cdot\hat{\mathbf{V}}|\Psi_J\rangle \\ &\quad - \frac{1}{2}\langle\Psi_{I(\mathrm{eq})}|\hat{\mathbf{Q}}^{s}|\Psi_{I(\mathrm{eq})}\rangle\cdot\langle\Psi_{I(\mathrm{eq})}|\hat{\mathbf{V}}|\Psi_{I(\mathrm{eq})}\rangle \\ &\quad - \frac{1}{2}\langle\Psi_J|\hat{\mathbf{Q}}^{f}|\Psi_J\rangle\cdot\langle\Psi_J|\hat{\mathbf{V}}|\Psi_J\rangle \qquad (7)\\ &= \langle\Psi_J|\hat{H}|\Psi_J\rangle + \mathbf{Q}^{s}_{I(\mathrm{eq})}\mathbf{V}_J + \frac{1}{2}\mathbf{Q}^{f}_J\mathbf{V}_J - \frac{1}{2}\mathbf{Q}^{s}_{I(\mathrm{eq})}\mathbf{V}_{I(\mathrm{eq})} \qquad (8)\end{aligned}$$

Using eq 6, however, is inconvenient in practice as each state is assigned a different effective Hamiltonian. This requires a separate self-consistent calculation for each state. The linear independence of higher excited states is difficult to ensure in this case.

We will instead favor the perturbative approach, as advocated by the authors of ref 26 in their corrected linear response (cLR) solvation model for TDDFT. In this case, the original nonlinear Schrödinger equation, eq 3 (using the reaction field of state $|\Psi_{I(\mathrm{eq})}\rangle$), is solved for all considered states. The uncorrected excited state energy is then

$$E_J = \langle\Psi_J|\hat{H} + \langle\Psi_{I(\mathrm{eq})}|\hat{\mathbf{Q}}^{s}|\Psi_{I(\mathrm{eq})}\rangle\cdot\hat{\mathbf{V}}|\Psi_J\rangle \tag{9}$$

and the remaining terms in eq 7 are just added as a perturbative correction. The free energy of the excited state J reads

$$\begin{aligned}\mathcal{G}_J^{\mathrm{noneq}} &= E_J - \frac{1}{2}\mathbf{Q}_{I(\mathrm{eq})}\mathbf{V}_{I(\mathrm{eq})} + \frac{1}{2}\mathbf{Q}^{f}_J\mathbf{V}_J \qquad (10)\\ &\quad + \frac{1}{2}\mathbf{Q}^{f}_{I(\mathrm{eq})}\mathbf{V}_{I(\mathrm{eq})} - \mathbf{Q}^{f}_{I(\mathrm{eq})}\mathbf{V}_J \\ &= E_J - \frac{1}{2}\mathbf{Q}_{I(\mathrm{eq})}\mathbf{V}_{I(\mathrm{eq})} \qquad (11)\\ &\quad + \frac{1}{2}(\mathbf{Q}^{f}_J - \mathbf{Q}^{f}_{I(\mathrm{eq})})(\mathbf{V}_J - \mathbf{V}_{I(\mathrm{eq})})\end{aligned}$$

For this equality to hold, $\mathbf{Q}^{f}_{I(\mathrm{eq})}\mathbf{V}_J = \mathbf{Q}^{f}_J\mathbf{V}_{I(\mathrm{eq})}$ was assumed.[26] For the COSMO approach, this relation is actually exact, see section 2.3. Introducing the uncorrected excitation energy (with respect to the equilibrated state)

$$\Delta E_{J,I(\mathrm{eq})} = E_J - E_{I(\mathrm{eq})} \tag{12}$$

where $E_{I(\mathrm{eq})} = \langle\Psi_{I(\mathrm{eq})}|\hat{H} + \langle\Psi_{I(\mathrm{eq})}|\hat{\mathbf{Q}}|\Psi_{I(\mathrm{eq})}\rangle\cdot\hat{\mathbf{V}}|\Psi_{I(\mathrm{eq})}\rangle$, analogous to eq 9, the vertical free energy difference between the two states is

$$\Delta\mathcal{G}_{J,I(\mathrm{eq})} = \Delta E_{J,I(\mathrm{eq})} + \frac{1}{2}(\mathbf{Q}^{f}_J - \mathbf{Q}^{f}_{I(\mathrm{eq})})(\mathbf{V}_J - \mathbf{V}_{I(\mathrm{eq})}) \tag{13}$$

which agrees with the result provided in ref 26.

2.2. Linear Response of the Solvent. So far, we have applied the formalism to one state at a time, even in the nonequilibrium situation. The only interaction between the final (nonequilibrated) state and the initial (equilibrium) state is through the slow part of the reaction field. A different formalism, leading to another kind of state interactions, can be developed with the aid of response theory.[23,43,46,47]

The starting point is again the nonlinear Schrödinger equation, eq 3, and we consider the theory for exact solutions of the Schrödringer equation first. A time-dependent perturbation $\hat{X}(t)$ is added to the Hamiltonian, and the time-dependent exact reference state (usually the ground state $|\Psi_0\rangle$, we will in the beginning also assume that this is the equilibrated state) is parametrized as

$$\begin{aligned}|\Psi_0(t)\rangle &= e^{i\hat{S}(t)}|\Psi_{0(\mathrm{eq})}\rangle, \\ \hat{S}(t) &= \sum_x s_x(t)\hat{\tau}_x + \sum_x s^*_x(t)\hat{\tau}^\dagger_x\end{aligned} \tag{14}$$

where the transfer operators

$$\hat{\tau} = |\Psi_x\rangle\langle\Psi_{0(\mathrm{eq})}| \tag{15}$$

excite into a (arbitrary) complete basis of states $\{|\Psi_x\rangle\}$ that are orthogonal to the reference state, $\langle\Psi_x|\Psi_{0(\mathrm{eq})}\rangle = 0$. More details about the derivation are given in the Appendix, section A.

One finally arrives at an eigenvalue equation for the transition into state $|\Psi_J\rangle$ (see ref 43)

$$\mathbf{G}^{[2]}\mathbf{c}_J = \mathbf{S}^{[2]}\mathbf{c}_J\omega_J \tag{16}$$

The c_J are the expansion coefficients that describe the excited state in terms of the transfer operators $|\Psi_J\rangle = \sum_x c_{x,J}\tau_x|\Psi_{0(\mathrm{eq})}\rangle$ and $\omega_J = E_J - E_0$ is the transition frequency, which is in atomic units equivalent to the excitation energy.

The metric $\mathbf{S}^{[2]}$ is of no importance for the following discussion, we only focus on the structure of the free energy matrix:

$$G^{[2]}_{xy} = E^{[2]}_{xy} + \mathbf{V}^{[2]}_{xy}\mathbf{Q}_{0(\mathrm{eq})} + \mathbf{V}^{[1]}_{x}\mathbf{Q}^{f,[1]}_{y} \tag{17}$$

dx.doi.org/10.1021/ct300763v | J. Chem. Theory Comput. 2013, 9, 977−994

where x and y range over all excited states. The contributions in eq 17 are

$$E^{[2]}_{xy} = \langle\Psi_x|\hat{H}|\Psi_y\rangle - \delta_{xy}\langle\Psi_{0(\mathrm{eq})}|\hat{H}|\Psi_{0(\mathrm{eq})}\rangle \tag{18}$$

$$\mathbf{V}^{[2]}_{xy} = \langle\Psi_x|\hat{\mathbf{V}}|\Psi_y\rangle - \delta_{xy}\langle\Psi_{0(\mathrm{eq})}|\hat{\mathbf{V}}|\Psi_{0(\mathrm{eq})}\rangle \tag{19}$$

$$\mathbf{V}^{[1]}_{x} = \langle\Psi_x|\hat{\mathbf{V}}|\Psi_{0(\mathrm{eq})}\rangle \tag{20}$$

$$\mathbf{Q}^{\mathrm{f},[1]}_{x} = \langle\Psi_x|\hat{\mathbf{Q}}^{\mathrm{f}}|\Psi_{0(\mathrm{eq})}\rangle \tag{21}$$

$$\mathbf{Q}_{0(\mathrm{eq})} = \langle\Psi_{0(\mathrm{eq})}|\hat{\mathbf{Q}}|\Psi_{0(\mathrm{eq})}\rangle \tag{22}$$

The last term of 17 is of particular interest. We note, that for COSMO $\mathbf{V}^{[1]}_x\mathbf{Q}^{\mathrm{f},[1]}_y = \mathbf{V}^{[1]}_y\mathbf{Q}^{\mathrm{f},[1]}_x$ holds, such that $G^{[2]}_{xy}$ remains Hermitian. The difference to the solvent terms in the energy expressions from the previous section are obvious: While, e.g. in eq 7 expectation values like $\langle\Psi_J|\hat{\mathbf{Q}}^{\mathrm{f}}|\Psi_J\rangle$ appear, the linear response approach introduces transition moments like $\langle\Psi_J|\hat{\mathbf{Q}}^{\mathrm{f}}|\Psi_{0(\mathrm{eq})}\rangle$.

In their investigation of the differences between the state-specific and linear response approaches within the CSM framework, Corni et al.[44] have shown that the excitation energy of a simplified, but explicitly quantum-mechanically treated model system (with two electronic states), is

$$\begin{aligned}\Delta E^{\mathrm{s}}_{10} = {} & \Delta E_{10} - (\mu_{11} - \mu_{00})g\mu_{00} \\ & - \frac{1}{2}g_e(0)(\mu_{00} - \mu_{11})^2 - g_{\mathrm{e}}(\omega_{01})\mu_{01}{}^2 \\ & - \frac{1}{2\pi}\int_0^\infty \mathrm{d}\omega\, g_{\mathrm{e}}(i\omega)(\alpha_1(i\omega) - \alpha_0(i\omega))\end{aligned} \tag{23}$$

Here, μ_{xy} are the dipole and transition dipole matrix elements of the solute and g and $g_{\mathrm{e}}(\omega)$ are the total solvent response functions and its purely electronic part, respectively. The solute's polarizability (for states 0 and 1) is denoted as $\alpha_x(\omega)$, and ω_{01} is the frequency associated with the transition. Comparing to eq 13, we note that $\Delta E_{J,I(\mathrm{eq})}$ is the counterpart of the first two terms in eq 23, and the third term is just the correction in the nonequilibrium model. The fourth term of eq 23 is the equivalent of the $\mathbf{V}^{[1]}_x\mathbf{Q}^{\mathrm{f},[1]}_y$ (for $x = y = 1$) which occurs in the linear response treatment. However, referring to the treatment of dispersion effects in earlier work,[16,48] Corni et al. argue that the sum of the last two terms in eq 23 should be regarded as dispersion. Hence, it was suggested to omit the linear response term in any CSM approach, as it goes beyond the pure electrostatic picture.[11,44]

In our view, the linear response term is not what is commonly understood as a (London-type) dispersion interaction; pure dispersion is represented in the last term of eq 23. Rather, the response term describes the excitonic coupling to the solvent molecules. We recall that the fast part of the reaction field response is proportional to the rotationally averaged dynamic molecular polarizability of the solvent (in the range of optical frequencies). The dynamic molecular polarizability is in turn related to electronic transitions on the solvent molecules according to the sum-overstates expression $\alpha(\omega) \propto 1/3\sum_I|\mu_{0I}|^2/(\omega - \omega_I)$, where μ_{0I} is the transition dipole of excitation I, and ω_I its transition frequency. Equivalent contributions have been described (in a more explicit framework) in the scope of subsystem DFT.[1]

Furthermore, the off-diagonal contributions to $G^{[2]}_{xy}$, explicitly $\mathbf{V}^{[1]}_x\mathbf{Q}^{\mathrm{f},[1]}_y$, describe a coupling between excitations x and y mediated by the solvent molecules. Effectively this indirect, solvent mediated interaction results in a screening of the direct interactions via the Coulomb operator. This is of particular interest for couplings between spatially separated excitations on different chromophores (excitonic couplings). Within the PCM model, this has been exploited earlier by Iozzi et al.[49] in a TDDFT based subsystem approach to the calculation of excitonic couplings. We hence argue that a CSM based implementation of solvation effects should contain both, the linear response contribution *and* the adaptation of the reaction field to the changed exited-state charge density, either in the equilibrium or the nonequilibrium case.

We will, in this work, also treat cases of long-lived excited states which are equilibrated with the solvent. Then, the question arises, how to apply the linear response formalism in these cases. Although it seems straightforward to replace the reference state $|\Psi_{0(\mathrm{eq})}\rangle$ by $|\Psi_{I(\mathrm{eq})}\rangle$ in the derivation above, this is usually neither a practical nor a physically correct solution. It is not practical, as many approximate methods for excited states that have been derived by response theory require a special choice as reference function (the ground state). And it is not physically correct, for instance when considering the excitonic coupling between two excited states (both nonequilibrated, but in the presence of a reaction field that is equilibrated with respect to a third excited state): The interaction between these two states will still be the coupling of a deexcitation $|\Psi_I\rangle \rightarrow |\Psi_0\rangle$ to an excitation $|\Psi_0\rangle \rightarrow |\Psi_J\rangle$, and the last term of eq 17 must remain unchanged in order to provide the appropriate dynamic screening of the excitonic coupling.

We will therefore use a generalization of the linear response formalism, which uses the ground state as reference state, $|\Psi_0\rangle$, but allows a different state to be the equilibrated with the solvent, $|\Psi_{I(\mathrm{eq})}\rangle$. For more details, see the Appendix, section A. The free energy matrix, eq 17, is generalized to

$$G^{[2]}_{xy} = E^{[2]}_{xy} + \mathbf{V}^{[2]}_{xy}(\mathbf{Q}^{\mathrm{s}}_{I(\mathrm{eq})} + \mathbf{Q}^{\mathrm{f}}_0) + \mathbf{V}^{[1]}_x\mathbf{Q}^{\mathrm{f},[1]}_y \tag{24}$$

with the new matrix elements defined as

$$\mathbf{Q}^{\mathrm{s}}_{I(\mathrm{eq})} = \langle\Psi_{I(\mathrm{eq})}|\hat{\mathbf{Q}}^{\mathrm{s}}|\Psi_{I(\mathrm{eq})}\rangle \tag{25}$$

$$\mathbf{Q}^{\mathrm{f}}_0 = \langle\Psi_0|\hat{\mathbf{Q}}^{\mathrm{f}}|\Psi_0\rangle \tag{26}$$

We obtain the same solvent response term as before, only the second term, the static contribution, changes to include the slow part of the reaction field of the equilibrated state. Obviously, eq 17 is recovered for $I = 0$.

We note, that the dynamic screening terms derived by the above formalism are correct for all photophysical processes that involve the ground state as initial or final state, like the excitonic coupling process mentioned above, or radiative $S_1 \rightarrow S_0$ transitions. The formalism, however, is not entirely correct for other processes like excited state absorption. This dependence on the choice of the reference state should not appear in a full quantum mechanical solvation theory; seemingly, it is a consequence of the nonlinear nature of the Hamiltonian when CSMs are applied, cf. also the discussion about the nonequivalence of state-specific and linear-response aproaches in ref 44.

2.3. Conductor-like Screening Model (COSMO). COSMO features rather simple boundary conditions to determine the screening charges that represent the reaction field.[15] The assumption is made that the solute is embedded in an ideal conductor, that is the dielectric constant is set to $\varepsilon =$

∞. The effective surface charges for each surface element $Q_i = Q(s_i)$ are obtained from

$$Q_i = -f(\varepsilon) \sum_k (A^{-1})_{ik} V_k \tag{27}$$

where the kernel A is defined as[15]

$$A_{ik} = \begin{cases} 1/(s_i - s_k) & \text{for } i \neq k \\ 3.8\sqrt{S_i} & \text{for } i = k \end{cases} \tag{28}$$

S_i is the area of segment i.

The dielectric character of the embedding medium is accounted for by scaling the charges with a factor

$$f(\varepsilon) = \frac{\varepsilon - 1}{\varepsilon + a} \tag{29}$$

where ε is the macroscopic dielectric constant and a is a constant usually chosen as $a = 1/2$ (as in the present implementation, other implementations use $a = 0$). The error of this approximation is small for strong dielectrics and within 10% for weak dielectrics, which in view of the overall accuracy of the model seems sufficient.[50,51]

For the treatment of nonequilibrated states, we need to split the surface charge operator into a slow and a fast component. In the COSMO approach, this translates into the introduction of two scaling factors. The one for the fast component is $f_f = f(n^2)$ where n is the refractive index, the high-frequency limit of the dielectric function $\varepsilon(\omega \to \infty) \to n^2$. Otherwise the same definition, eq 29, is used. The slow component is consequently $f_s = f(\varepsilon) - f(n^2)$.

2.4. Notation in Second Quantization. In second quantization the normal ordered Hamiltonian of the isolated molecule reads

$$\hat{H} = E_0 + \hat{H}_N = E_0 + \hat{F}_N + \hat{G}_N \tag{30}$$

where normal order refers to the Fermi vacuum defined by the reference determinant $|0\rangle$ (particle-hole formalism). The contributions to $\hat{H}$ are defined as

$$E_0 = \langle 0|\hat{H}|0\rangle, \qquad \hat{F}_N = f_p^q a_q^p, \qquad \hat{G}_N = \frac{1}{4} g_{pr}^{qs} a_{qs}^{pr} \tag{31}$$

E_0 is the expectation value of the vacuum Hamiltonian, f_p^q is the Fock matrix, and $g_{pr}^{qs} = \langle qs||pr\rangle$ are the antisymmetrized two-electron repulsion integrals. The operators a_q^p and a_{qs}^{pr} are normal-ordered and hence fulfill $\langle 0|a_q^p|0\rangle = 0$ and $\langle 0|a_{qs}^{pr}|0\rangle = 0$. They consist of the primitive spin−orbital annihilation and creation operators a_p and a^p. The Einstein summation convention over repeated upper and lower indices is assumed in all equations unless explicit summation signs appear. We will employ the usual convention that p, q, ... enumerate general spin−orbitals, while i, j, ... refer to orbitals occupied in the reference determinant $|0\rangle$, and a, b, ... refer to unoccupied (virtual) orbitals. The spin−orbitals $|\phi_p\rangle$ (which form an orthogonal set) are spanned by a (nonorthogonal) set of basis functions $|\chi_\mu\rangle$, with $|\phi_p\rangle = \sum_\mu C_{\mu p}|\chi_\mu\rangle$.

In order to represent the solvent interactions in this formalism, the density matrix of a state $|\Psi\rangle$ is introduced as

$$P_q^p[|\Psi\rangle] = \langle \Psi|a_q^p|\Psi\rangle \tag{32}$$

Note that the definition of one-particle densities in actual computational methods slightly deviates from this straightforward definition. In the following, it is always understood that $P_p^q[|\Psi\rangle]$ is evaluated according to the prescriptions for the method under consideration. Back-transformed to the contravariant basis set representation, $P_\mu^\nu = \sum_{pq} P_p^q C_{\mu p} C_{\nu q}$, the density matrix serves to write down the elements of the molecular potential on the cavity surface in the following manner:

$$V_i = V_{i,\mathrm{nuc}} + \sum_{\mu\nu} (V_i)_\nu^\mu P_\mu^\nu[|\Psi\rangle] \tag{33}$$

The explicit expressions for contributions from nuclei (with charge Z_I) and electrons are given by

$$V_{i,\mathrm{nuc}} = \sum_I \frac{Z_I}{|\mathbf{R}_I - \mathbf{s}_i|}, \qquad (V_i)_\nu^\mu = \left\langle \chi_\mu \middle| \frac{-1}{|\mathbf{r} - \mathbf{s}_i|} \middle| \chi_\nu \right\rangle \tag{34}$$

Furthermore, we introduce the following matrix elements: The interaction of the nuclear charges with the reaction field induced by themselves,

$$j_{\mathrm{nuc}} = \mathbf{Q}_{\mathrm{nuc}} \cdot \mathbf{V}_{\mathrm{nuc}} \tag{35}$$

the interaction of the nuclear charges with the reaction field induced by the electronic charge distribution $\chi_\mu\chi_\nu$ and vice versa,

$$j_\nu^\mu = \mathbf{Q}_{\mathrm{nuc}} \cdot \mathbf{V}_\nu^\mu + \mathbf{Q}_\nu^\mu \cdot \mathbf{V}_{\mathrm{nuc}} = 2\mathbf{Q}_{\mathrm{nuc}} \cdot \mathbf{V}_\nu^\mu \tag{36}$$

and finally the interaction of the electronic charge distribution $\chi_\mu\chi_\nu$ with the reaction field induced by the charge distribution $\chi_\kappa\chi_\lambda$,

$$B_{\nu,\lambda}^{\mu,\kappa} = \mathbf{Q}_\nu^\mu \mathbf{V}_\lambda^\kappa \tag{37}$$

Note that the latter quantity has the symmetry property $B_{\nu,\lambda}^{\mu,\kappa} = B_{\lambda,\nu}^{\kappa,\mu}$ but that, in general, $B_{\nu,\lambda}^{\mu,\kappa} \neq B_{\lambda,\nu}^{\mu,\kappa}$, as indicated by the comma between the indices. Unlike the two-electron repulsion integrals, see eq 31, $B_{\nu,\lambda}^{\mu,\kappa}$ is never used in antisymmetrized form. Equations 35−37 have been written in the covariant basis function representation but can easily be transformed to the spin−orbital (MO) basis via the coefficients $C_{\mu p}$.

Using this notation, the total energy of the solvated reference state $|0\rangle$ reads

$$\begin{aligned} E_{0,\mathrm{solv}} &= E_0 + \langle 0|\langle \Psi_{I(\mathrm{eq})}|\hat{\mathbf{Q}}|\Psi_{I(\mathrm{eq})}\rangle \hat{\mathbf{V}}|0\rangle \\ &= E_0 + j_{\mathrm{nuc}} + \sum_k j_k^k + \sum_{k,pq} B_{k,p}^{k,q} P_q^p[|\Psi_{I(\mathrm{eq})}\rangle] \end{aligned} \tag{38}$$

where $P_q^p[|\Psi_{I(\mathrm{eq})}\rangle] = \langle \Psi_{I(\mathrm{eq})}|a_q^p|\Psi_{I(\mathrm{eq})}\rangle$ is the one-particle density of the equilibrated state. Note that we deviate from the usual formalism and include here a general state $|\Psi_{I(\mathrm{eq})}\rangle$ with respect to which the solvent is equilibrated.

We also introduce the free reference energy

$$\mathcal{G}_0 = E_{0,\mathrm{solv}} - \frac{1}{2}\mathbf{Q}_{I(\mathrm{eq})}\mathbf{V}_{I(\mathrm{eq})} \tag{39}$$

The augmented Fock operator that is diagonalized during the *self-consistent field* (SCF) procedure has the following structure

$$\hat{F}_{N,\mathrm{solv}} = (f_p^q + j_p^q + B_{p,s}^{q,r} P_r^s[|\Psi_{I(\mathrm{eq})}\rangle])a_q^p \tag{40}$$

and contains the vacuum Fock matrix element f_p^q and the additional solvation terms.

dx.doi.org/10.1021/ct300763v | J. Chem. Theory Comput. 2013, 9, 977−994

3. CONTINUUM SOLVATION APPLIED TO CIS AND ADC(2)

3.1. CIS Method. The configuration interaction with singly excited determinants (CIS) is one of the most simple approaches to treat excited states. We include it into the discussion, as the actual method under consideration, ADC(2), may be viewed as degenerate perturbation theory with the CIS wave functions as zeroth-order states[34] (or taking another perspective: The CIS excitation energies are equivalent to those of the ADC(1) method[33]). Hence, all terms that appear in CIS do also appear in ADC(2), and we will use the more simple structure to analyze the additional terms due to the solvation model (in particular those that appear in the linear response formalism) and generalize these to the more complex ADC(2) method.

The ground state wave function in the CIS method is the Hartree−Fock determinant. The excited states are expanded as linear combinations of singly excited determinants, here notated as excitation operator acting on the Hartree−Fock reference determinant:

$$|\Psi_J^{\mathrm{CIS}}\rangle = (R^{(J)})_a^i a_i^a |0\rangle = \hat{R}_1^{(J)}|0\rangle \tag{41}$$

For the sake of legibility, we will omit the excited state index J in the following unless it is necessary to distinguish different excited states. The coefficients R_a^i are determined from the secular equations

$$A_{aj}^{ib} R_b^j = \omega R_a^i \tag{42}$$

and the explicit form of the matrix-vector product on the left-hand side reads

$$\rho_a^i = A_{aj}^{ib} R_b^j = \langle 0|a_i^a \hat{H}_N \hat{R}_1|0\rangle = (\varepsilon_a - \varepsilon_i) R_a^i + g_{aj}^{ib} R_b^j \tag{43}$$

The transition densities are identical to the coefficients of the excitation operators,

$$\gamma_q^p = \langle 0|a_q^p \hat{R}_1|0\rangle = R_a^i \delta_q^a \delta_i^p \tag{44}$$

Direct application of eq 32 to a CIS state gives the "unrelaxed" density

$$\tilde{P}_q^p = \langle 0|\hat{R}_1^\dagger a_q^p \hat{R}_1|0\rangle = \begin{cases} \tilde{P}_j^i = -R_c^i R_j^c \\ \tilde{P}_b^a = R_b^k R_k^a \\ \tilde{P}_i^a = \tilde{P}_a^i = 0 \end{cases} \tag{45}$$

The unrelaxed density still misses the contribution from the orbital response. These terms add an additional contribution to the virtual-occupied block (and its Hermitian conjugate) resulting in the relaxed density,

$$P_i^a = (P^\dagger)_i^a = \tilde{P}_i^a + Z_i^a \tag{46}$$

where Z_i^a is the solution of the "Z-vector" equations[52]—or coupled-perturbed Hartree−Fock (CPHF) equations—for the state in question (see Appendix, section B).

3.2. ADC(2) Method. The algebraic diagrammatic construction through second-order, ADC(2), was first introduced by Schirmer.[33] Later,[34] its close relation to CIS(D_∞),[53] a degenerate perturbation theory variant of CIS(D),[54] and to CC2, the second-order approximate coupled-cluster singles and doubles model,[35] was realized.

The method directly considers excitation energies without reference to a specific ground state, but it seems justified to use second-order Møller-Plesset perturbation theory (MP2) for that purpose, if total energies are required, for instance for determining excited state equilibrium structures. The MP2 energy is evaluated as

$$E^{(0)} + E^{(1)} + E^{(2)} = E_0 + \frac{1}{4} t_{ab}^{ij} g_{ij}^{ab} \tag{47}$$

assuming the Brillouin condition to hold ($f_i^a = 0$). For canonical orbitals, $f_q^p = \delta_q^p \varepsilon_q$, and the first order amplitudes are given by

$$t_{ab}^{ij} = -g_{ab}^{ij}/(\varepsilon_a + \varepsilon_b - \varepsilon_i - \varepsilon_j) \tag{48}$$

We usually collect the amplitudes in an operator $\hat{T}_2 = {}^1/_4 t_{ab}^{ij} a_{ij}^{ab}$.

With some caution, the ADC(2) excited state can be thought as single and double excitation operators acting on the ground state wave function (up to first-order),

$$\Psi_J^{\mathrm{ADC(2)}} = (\hat{R}_1^{(J)} + \hat{R}_2^{(J)})(1 + \hat{T}_2)|0\rangle \tag{49}$$

Note that this equation only sketches the basic structure of the wave function ansatz. All further equations to be derived for ADC(2) use the additional condition that they are consistently truncated at second-order and exclude disconnected contributions in order to maintain size-extensivity.[33] As above for the CIS case, we will omit the excited state index J in all further equations, unless absolutely necessary.

The original derivation of ADC(2)[33] starts from the polarization propagator. In the course of that derivation, an eigenvalue problem for the determination of the excited states is obtained that has the general structure of eq 16. Approximations to $E^{[2]}$ and $S^{[2]}$ are then based on perturbation theory and comparison to the diagrammatic expansion of the polarization propagator. It follows that the excitation energies and transition vectors are determined by solving

$$\begin{pmatrix} A_{ak}^{ic} & A_{akl}^{icd} \\ A_{abk}^{ijc} & A_{abkl}^{ijcd} \end{pmatrix} \begin{pmatrix} R_c^k \\ R_{cd}^{kl} \end{pmatrix} = \omega \begin{pmatrix} R_a^i \\ R_{ab}^{ij} \end{pmatrix} \tag{50}$$

The corresponding matrix-vector products are

$$\begin{aligned} \rho_a^i &= A_{ak}^{ic} R_c^k + A_{akl}^{icd} R_{cd}^{kl} \\ &= \langle 0|a_i^a \left[\hat{H}_N + \frac{1}{2}[\hat{H}_N, \hat{T}_2] + \frac{1}{2}[\hat{T}_2^\dagger, \hat{H}_N], \hat{R}_1 \right]|0\rangle \\ &\quad + \langle 0|a_i^a \hat{H}_N \hat{R}_2|0\rangle \end{aligned} \tag{51}$$

$$\rho_{ab}^{ij} = A_{abk}^{ijc} R_c^k + A_{abkl}^{ijcd} R_{cd}^{kl} = \langle 0|a_{ij}^{ab} \hat{H}_N \hat{R}_1|0\rangle + \langle 0|a_{ij}^{ab} \hat{F}_N \hat{R}_2|0\rangle \tag{52}$$

The explicit expressions are given in Table 1. The term group eq 1-A is again the CIS expression, cf. eq 42. The expressions for the double excitations are consistently truncated at second-order (the "strict" ADC(2) variant[33]) which allows, for given R_1, to calculate R_2 by direct inversion.[34]

In the original definition of ADC(2),[33,55] the transition density has to be evaluated strictly through second-order, which requires the computationally expensive and thus undesirable calculation of certain parts of the second-order wave function. In this work, we will therefore use a modified expression, in which these terms are neglected. This may be justified by the analogy to coupled-cluster response theory, in which

Table 1. Explicit Expressions of the ADC(2) Working Equations[a]

$$\rho_a^i = (\varepsilon_a - \varepsilon_i)R_a^i + g_{ak}^{ic}R_c^k \quad (1\text{-A})$$

$$+\frac{1}{2}(g_{ac}^{ik}(t^\dagger)_{kl}^{cd}R_d^l + t_{ac}^{ik}g_{kl}^{cd}R_d^l) \quad (1\text{-B})$$

$$+\frac{1}{2}\left(\frac{1}{2}g_{kl}^{cd}t_{ad}^{kl}R_c^i + \frac{1}{2}(t^\dagger)_{kl}^{cd}g_{ad}^{kl}R_c^i\right) - \frac{1}{2}\left(\frac{1}{2}g_{kl}^{cd}t_{cd}^{il}R_a^k - \frac{1}{2}(t^\dagger)_{kl}^{cd}g_{cd}^{il}R_a^k\right) \quad (1\text{-C})$$

$$+\frac{1}{2}g_{al}^{cd}R_{cd}^{il} + \frac{1}{2}g_{id}^{kl}R_{kl}^{ad} \quad (1\text{-D})$$

$$\rho_{ab}^{ij} = g_{ab}^{cj}R_c^i + g_{ab}^{ic}R_c^j + g_{kb}^{ij}R_a^k + g_{ak}^{ij}R_b^k \quad (2\text{-A})$$

$$+(\varepsilon_a + \varepsilon_b - \varepsilon_i - \varepsilon_j)R_{ab}^{ij} \quad (2\text{-B})$$

[a]The Brillouin condition $f_i^a = 0$ and canonical orbitals $f_q^p = \delta_q^p\varepsilon_p$ are assumed. The symbols for term groups are given for later reference.

perturbation theory motivated truncations are applied to the stationary energy functional, while incomplete (in the sense of a perturbation expansion) expressions are accepted for derived quantities, e.g., for transition moments. With this restriction we obtain the following expression for the transition moment

$$\gamma_q^p = \langle 0|a_q^p\hat{R}_1|0\rangle + \langle 0|\hat{T}_1^\dagger a_q^p\hat{R}_1|0\rangle + \langle 0|\hat{T}_2^\dagger a_q^p\hat{R}_2|0\rangle + \langle 0|\hat{T}_2^\dagger a_q^p\hat{R}_1T_2|0\rangle \quad (53)$$

or explicitly

$$\gamma_j^i = -\frac{1}{2}(t^\dagger)_{jl}^{cd}R_{cd}^{il} \quad (54)$$

$$\gamma_a^i = R_a^i - \frac{1}{2}(t^\dagger)_{kl}^{cd}t_{ad}^{kl}R_c^i + \frac{1}{2}(t^\dagger)_{kl}^{cd}t_{cd}^{il}R_a^k \quad (55)$$

$$\gamma_i^a = (t^\dagger)_{ik}^{ac}R_c^k \quad (56)$$

$$\gamma_b^a = \frac{1}{2}(t^\dagger)_{kl}^{ad}R_{bd}^{kl} \quad (57)$$

We note that the R_a^i contribution is zeroth-order in the perturbation expansion, and $(t^\dagger)_{ik}^{ac}R_c^k$ is first-order, while the remaining contributions are second-order terms.

The definition of unrelaxed and relaxed excited state densities is somewhat more involved. An overview is given in the Appendix. We will throughout this work use relaxed densities. With respect to the original formulation of ADC(2), the same comments apply as for the transition moments. We note, however, that the relaxed densities as defined in ref 34 are strictly consistent with gradient theory.

3.3. State-Specific Self-Consistent Reaction Field Approach. In the state-specific approach, the self-consistent reaction field of a selected state is determined, either the electronic ground state or any excited state. In the terminology of section 2 this is the state $|\Psi_{I(\mathrm{eq})}\rangle$. In order to achieve this, the solution of the Hartee-Fock (HF) equations and, in our case, the determination of the MP2 ground state or ADC(2) excited state energy and corresponding relaxed density is iterated until the surface charges obtained from the latest relaxed density equal the previous ones, within a numerical threshold. Similar procedures have been reported for ground-state MP2, also known as PTED scheme—for perturbation theory (PT) with self-consistent reaction field energy (E) and density (D)[51,56,57]—and CCSD,[29,30] in the latter case also including the excited state case using the equation-of-motion (EOM) approach.

We note that we prefer relaxed densities, in contrast to other work, e.g. ref 29. In particular for ADC(2), this avoids some arbitrariness in the definition of excited state densities.[58] The relaxed density has a straightforward definition as analytic derivative of the excited state energy with respect to an external one-particle perturbation. The impact on computation time is moderate, as solving the CPHF equations has a lower computational scaling than the remaining part of the ADC(2) method.

Regarding MP2, some objections have been raised against the PTED scheme.[59] It was pointed out that the PTED scheme is formally not consistent with a pure second-order treatment of electron correlation. While we agree with this viewpoint and also recognize that previous numerical experience[57,59] does not favor the iterative scheme over the noniterative PTE scheme (which uses the reaction field calculated from the HF density), we have to recall that our main target is to treat *excited* states. Obviously, the HF density does not provide a proper description of the excited state charge distribution, and the most straightforward solution is thus to base the method on a self-consistent excited state reaction field.

Once the HF equations are solved in the presence of the reaction field of $|\Psi_{I(\mathrm{eq})}\rangle$, all solvent contributions are contained in $F_{N,\mathrm{solv}}$, eq 40. Hence, the expressions for the correlation and excitation energies remain unaltered compared to the in vacuo case, with F_N replaced by $F_{N,\mathrm{solv}}$ and E_0 replaced by $\mathcal{G}_0$. We particularly note that F_N can be chosen diagonal (canonical) such that T_2 and R_2 can be obtained by direct inversion, see, e.g., eq 48. No storage of these quantities in necessary then, which makes the implementation of MP2 and ADC(2) applicable to very large systems.[41]

The expressions for the CPHF equations remain unaltered, too. This is because we assume in their derivation that the reaction field due to the correlated density is a fixed external field during the HF iterations. In this case, the reaction field only modifies the one-particle contributions to the Fock matrix. Taking the derivative of the HF energy expression with respect to the orbital rotation parameters then gives exactly the same expressions as for the in vacuo case.

This procedure leads to properties, e.g. dipole moments, which are consistent with finite difference calculations that probe the response of the *solute alone* in the presence of a fixed reaction field. This defines purely molecular properties which only depend on the solute and exclude the spurious direct contribution from the polarization of the cavity surface charges. For additional comments, see Appendix, section B.

If molecular geometric gradients are targeted, the additional cavity terms are needed, however, and the entire PTED scheme becomes a bit cumbersome, as the relaxed density that enters into the HF equations is perturbation-dependent, too. The situation is less involved in case of the PTE-scheme for MP2.[60] In this case, an additional term appears in the CPHF equations, which depends on the *B*-matrix.

Turning back to the iterative scheme used in this work, once the iterations are converged, the free energy of the equilibrated state is simply

$$\mathcal{G}_{I(\mathrm{eq})} = \mathcal{G}_0 + \Delta E_{\mathrm{corr+exc}}^{(I)} \quad (58)$$

where $\Delta E^{(I)}_{\mathrm{corr+exc}}$ collects the correlation (and excitation) energy contributions. $\mathcal{G}_0$ is given in eq 39, and $\Delta E^{(I)}_{\mathrm{corr+exc}} = {}^1/_4 t^{ij}_{ab} g^{ij}_{ab} + \omega_I$, where ω_I is the eigenvalue determined by eq 50.

For the states which are not in equilibrium with the solvent, we use the perturbative correction, eq 13. The free energy of a nonequilibrium state is then

$$\mathcal{G}^{\mathrm{noneq}}_J = \mathcal{G}_0 + \Delta E^{(I)}_{\mathrm{corr+exc}} + \Delta E_{J,I(\mathrm{eq})} + \frac{1}{2}(\mathbf{Q}^{\mathrm{f}}_J - \mathbf{Q}^{\mathrm{f}}_{I(\mathrm{eq})})(\mathbf{V}_J - \mathbf{V}_{I(\mathrm{eq})}) \tag{59}$$

where we have split the energy into $\Delta E^{(I)}_{\mathrm{corr+exc}}$ and $\Delta E_{J,I(\mathrm{eq})}$, the former being the sum of correlation and excitation energy of the equilibrated state, while the latter is the vertical energy difference to the nonequilibrated state. Comparison with eq 58 makes it obvious that ${}^1/_2(\mathbf{Q}^{\mathrm{f}}_J - \mathbf{Q}^{\mathrm{f}}_{I(\mathrm{eq})})(\mathbf{V}_J - \mathbf{V}_{I(\mathrm{eq})})$ is a correction of the vertical excitation energy relative to the equilibrated state; see also eq 13.

3.4. Solvent Response Terms. The linear-response ansatz applied to a HF ground state gives the time-dependent HF equations (due to the formal equality also denoted as random-phase approximation, RPA).[61] Neglect of the coupling between excitations and deexcitations leads to the Tamm−Dancoff approximation which is equivalent to CIS. As indicated in secion 2.2, the linear response of the CSM leads to a term $\mathbf{V}^{[1]}_x \mathbf{Q}^{\mathrm{f},[1]}_y$; see eq 17. For CIS, we can identify

$$\mathbf{V}^{[1]}_x = \langle 0|a^i_a \hat{\mathbf{V}}|0\rangle = \mathbf{V}^i_a \tag{60}$$

$$\mathbf{Q}^{[1]}_y = \langle 0|\hat{\mathbf{Q}} a^b_j|0\rangle = \mathbf{Q}^b_j \tag{61}$$

and, hence, comparing to eq 37

$$\mathbf{V}^{[1]}_x \mathbf{Q}^{\mathrm{f},[1]}_y = \mathbf{V}^i_a \mathbf{Q}^b_j = B^{i,b}_{a,j} \tag{62}$$

The matrix-vector product, eq 43, is consequently modified to

$$\rho^i_a = (\varepsilon_a - \varepsilon_i) R^i_a + (g^{ib}_{aj} + B^{i,b}_{a,j}) R^j_b \tag{63}$$

The other solvent-dependent term in eq 17, $\mathbf{V}^{[2]}_{xy}\mathbf{Q}_{\omega(\mathrm{eq})}$ can be identified as the contribution from the equilibrium reaction field. These are included in the Fock operator $\hat{F}_{N,\mathrm{solv}}$ (see eq 40) and appears in eq 63 as modified orbital energies ε_p.

As indicated, the solvent response term has the same structure as the two-electron contribution $g^{ib}_{aj} R^j_b$. As a physical interpretation, $B^{i,b}_{a,j}$ describes a screening of the Coulomb interaction between different excited states $|\Psi^{\mathrm{CIS}}_J\rangle$ and $|\Psi^{\mathrm{CIS}}_K\rangle$. The Coulomb contribution to the matrix element between the states is then $(R^{(J)})^a_i (g^{i,b}_{a,j} + B^{i,b}_{a,j})(R^{(I)})^j_b$, whereas the exchange contribution, $R^{(J)})^a_i g^{b,i}_{a,j} (R^{(I)})^j_b$, is not screened. This has three consequences: (a) The screening allows for self-interaction (if $J = K$), which is physically correct. It accounts for the nonresonant coupling of the molecule's transition density with the excited states of surrounding solvent molecules, represented by the response kernel of the continuum, $B^{i,b}_{a,j}$. This is a long-range interaction and particularly pronounced for molecules with a large transition dipole moment. (b) For triplet excited states ($R^a_i = -R^{\bar{a}}_{\bar{i}}$, where a bar denotes β spin), the screening term vanishes after spin summation. This is also acceptable, as triplet excited states have only short-range resonance interactions due to the exchange term. (c) For charge-transfer states (consider a single element of the excitation vector R^a_i with orbital a and i localized on different parts of the molecule) the Coulombic interaction of electron and hole (originating from the exchange term $R^a_i g^{a,i}_{a,i} R^i_a$) remains unscreened. The latter is possibly the main source of error for the pure linear response approach. In this work, we will account for it by the state-specific procedure as outlined in section 3.3, either in the equilibrium or nonequilibrium formalism.

Moving to the ADC(2) equations, we can again start from eqs 16 and 17. As discussed above, the first of the two solvent-dependent terms in eq 17 enters through the modified Fock operator, while the second describes the screened interaction between the transition densities of the excited states. Using the construction principle of ADC(2), we expand the matrix elements to first-order

$$(V^{[1]}_x)^{(1)} = \langle 0|a^i_a \hat{\mathbf{V}}(1 + \hat{T}_2)|0\rangle = \mathbf{V}^i_a + \mathbf{V}^c_k t^{ik}_{ac} \tag{64}$$

$$(Q^{[1]}_y)^{(1)} = \langle 0|(1 + T^\dagger_2)\hat{\mathbf{Q}} a^b_j|0\rangle = \mathbf{Q}^b_j + (t^\dagger)^{bc}_{jk}\mathbf{Q}^k_c \tag{65}$$

The operator $\hat{T}_2$ originates from the perturbation expansion of the ground state, all other terms that may arise from the perturbation expansion of the excited state do not give any first-order contribution to the matrix elements. Upon assembling the final expression, we have to make sure to truncate strictly at second-order. In particular, we have to regard the interaction kernel of the solvation model (connecting $\mathbf{V}$ and $\mathbf{Q}$; see eq 27) as first-order in the perturbation expansion (as it describes an electron−electron interaction, too). We thus obtain

$$(\mathbf{V}^{[1]}_x \mathbf{Q}^{f,[1]}_y)^{(2)} = B^{i,b}_{a,j} + B^{c,b}_{k,j} t^{ik}_{ac} + (t^\dagger)^{bc}_{jk} B^{i,k}_{a,c} \tag{66}$$

The first term is equivalent to the CIS expression, see eq 63, and implements the screening of the respective term in the ADC(2) eigenvalue problem; see Table 1 (term eq 1A). The other two terms contribute to the matrix-vector product as

$$\rho^i_a \leftarrow \frac{1}{2}(B^{i,k}_{a,c}(t^\dagger)^{cd}_{kl} R^l_d + t^{ik}_{ac} B^{c,d}_{k,l} R^l_d) \tag{67}$$

This is the screening contribution to the terms summarized as eq 1B in Table 1. No further terms of this type arise, which underlines that our above derivation is consistent with the structure of the ADC(2) eigenvalue problem.

For the determination of the relaxed one-particle density, a set of further terms occurs for the right-hand side of the CPHF equations. These terms arise from the energy contributions due to eqs 63 and 67. Detailed expressions are given in the Appendix.

3.5. Implementation. Our implementation is based on the CIS and ADC(2) schemes implemented in the RICC2 module[41] of the TURBOMOLE package,[42] which makes use of the resolution of the identity trick to enhance the speed of integral transformations (for further details, see ref 41). The basic routines implementing COSMO were already available, too.[50,51]

The calculation of the additional terms described in section 3.4, eqs 63 and 67, only requires an insignificant amount of CPU time. The only effort consists in retrieving the excitation vectors R^i_a or the intermediates $C^a_i = (t^\dagger)^{ac}_{ik} R^k_c$ and performing the transformation with $B^{i,b}_{a,j}$ in an integral direct way, using the existing implementation of this step.[50,51] The second term in eq 67 is implemented by adding the result of $B^{c,d}_{k,l} R^l_d$ (which is the same as $B^{k,d}_{c,l} R^l_d$ due to the symmetry properties of the B matrix) to the intermediate $\overline{F}^c_k = g^{cd}_{kl} R^l_d$. The result is then contracted with t^{ik}_{ac}, just as in the standard algorithm without solvent dependent terms.[41]

The only significant additional time requirements stem from the iterative solution of the self-consistency problem for the reaction field which is implemented by an outer loop over the SCF program and the correlation and excited state treatment in the RICC2 module.

4. SAMPLE APPLICATIONS

The molecular systems considered in this section are shown in Scheme 1. Cartesian coordinates are provided as Supporting Information. We will, particularly for systems **1** and **1a**, discuss the influence of linear response and state-specific terms and give an idea of the capabilities and limitations of the approach. Systems **2** and **3** serve to demonstrate the screening of resonance interactions due to a polarizable environment, while the application to system **4** concerns the solvent dependence of intramolecular charge transfer states.

Scheme 1. Structures of the Investigated Molecules

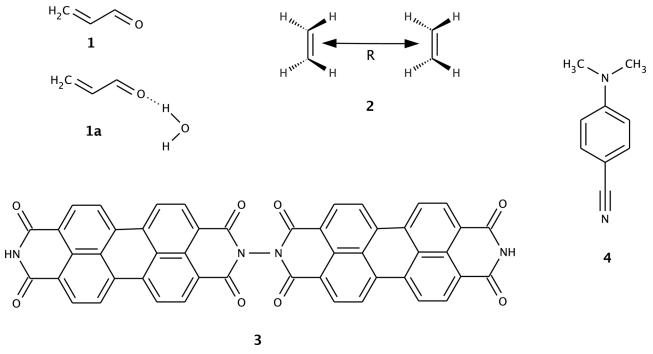

4.1. Acrolein. The acrolein molecule, **1**, has been discussed in a number of previous works.[6,26,29,31,62] The molecule shows two valence transitions, the energetically lower one has $n-\pi^*$ character and the upper one has $\pi-\pi^*$ character. The transitions also differ significantly in the magnitude of their transition dipole moments and the change of the dipole moment in the excited state. This, particularly, renders the molecule interesting for discussing the influence of linear-response and state-specific terms, section 4.1.1. We will also discuss basis set effects and the influence of cavity parameters, section 4.1.2, and compare to experiment and previous theoretical work in section 4.1.3. Unless noted otherwise, we employ the MP2/TZVPP in vacuo structure.

4.1.1. Breakdown of the Contributions to the Solvent Shift of Excitation Energies. We calculated the ADC(2)/TZVPP vertical excitation energies at a fixed molecular geometry. These calculations were performed for the isolated molecule and with COSMO embedding, using two sets of parameters, $\varepsilon = 2.2$, $n = 1.42$ to simulate a nonpolar solvent (such as 1,4-dioxane), and $\varepsilon = 37.5$, $n = 1.34$ representing a strongly polar solvent (acetonitrile). The resulting changes in the vertical excitation energies are visualized in Figure 1.

In Figure 1, we always start with the in vacuo excitation energy, and in a first step, we include the solvent effect introduced by the modified Hamiltonian. Without linear response terms, only the Fock operator changes according to eq 40. The linear response terms introduce an additional screening of the Coulomb interactions; see eq 63 for the CIS contribution and eq 67 for the correlation contributions in ADC(2).

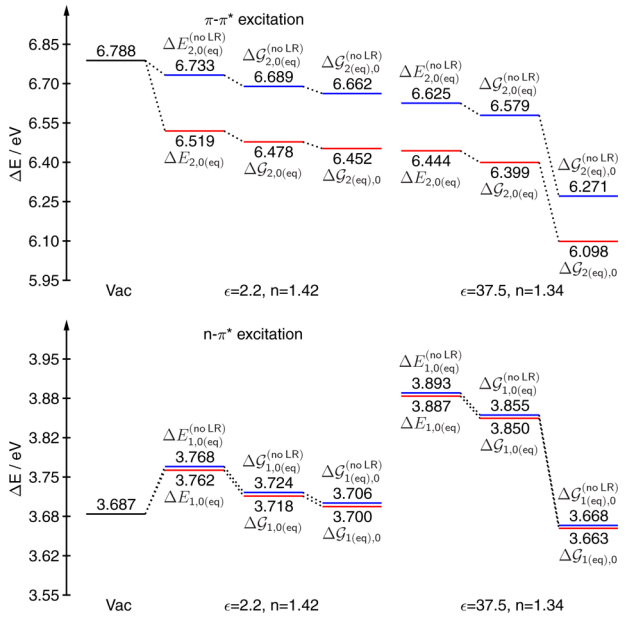

Figure 1. Breakdown of the various contributions in the COSMO solvation model for the acrolein molecule: Vertical excitation energies $\Delta E_{I,0(\mathrm{eq})}$ and corrected free energy differences $\Delta\mathcal{G}_{I,0(\mathrm{eq})}$, cf. eq 13, of the $\pi-\pi^*$ transition (upper panel) and the $n-\pi^*$ transition (lower panel), calculated at the ADC(2)/TZVPP level. "(no LR)" indicates that the linear response contributions from the solvent have been neglected; see also section 2.2. The last bar in each series corresponds to a vertical energy separation when the reaction field is relaxed for the excited state, $\Delta\mathcal{G}_{I(\mathrm{eq}),0}$.

The change in the Fock operator may either lower the excitation energy (in case of the $\pi-\pi^*$ transition) or raise it ($n-\pi^*$ transition). This effect depends on the sign of the interaction between the ground state reaction field (which up to the present step remains unchanged) and the charge distribution of the difference density. For the $\pi-\pi^*$ transition, the dipole moment direction remains basically the same, but its modulus becomes stronger, which explains the lowering of the excitation energy. The $n-\pi^*$ transition, in contrast, is associated with a decrease of the dipole moment and a change of its direction, leading to a net increase of the excitation energy, as the excited state interacts less favorable with the ground state reaction field, compared with the ground state.

The additional linear response terms always lower the excitation energy. The transition density interacts with the response of the reaction field induced by itself and hence is always aligned optimally. The transition moment of the $\pi-\pi^*$ transition is much larger than the weakly allowed $n-\pi^*$ transition, and consequently, we find a considerable shift of the $\pi-\pi^*$ transition by 0.2 eV, whereas the effect is vanishingly small for the $n-\pi^*$ excitation; see Figure 1.

In the next step, we also account for the response of the fast component of the reaction field according to the change of the charge distribution, cf. eq 13. Again, this term always leads to an energy lowering. In the present example, this amounts to about 0.05 eV in both cases.

Finally, we report in Figure 1 the effect of equilibrium solvation for the excited state ($\Delta\mathcal{G}_{I(\mathrm{eq}),0}$). In this step, the excited state is further stabilized, whereas the ground-state rises in energy (not visible in Figure 1 as only vertical energy differences are reported). The correction due to the fast degrees

dx.doi.org/10.1021/ct300763v | J. Chem. Theory Comput. 2013, 9, 977−994

of freedom, eq 13, is applied again, this time, however, with the excited state as the equilibrated state and the ground state as nonequilibrium state. As expected the transition from nonequilibrium solvation to equilibrium solvation for the excited state has the strongest effect for a polar solvent. The differences between $\Delta\mathcal{G}_{I,0(\mathrm{eq})}$ and $\Delta\mathcal{G}_{I(\mathrm{eq}),0}$ also underline that the prediction of solvent shifts of fluorescence bands requires to take into account the equilibration of the excited state.

Overall, the results indicate that both types of terms, those emerging from the linear response picture and those from a state-specific approach can give significant contributions. Neither beforehand nor in hindsight is there a reason to neglect either and we argue that both should be included (compare also the formal arguments given in section 2.2). Whether the inclusion of these terms improves agreement with experiment (or at least not deteriorates the performance) will be discussed below for the vacuum to solvent shift of acrolein in aqueous phase.

4.1.2. Basis Set Dependence and Influence of Cavity Construction Parameters. The basis set truncation error is investigated for a series of basis sets, SVP, TZVP, TZVPP, and QZVPP, as available in the TURBOMOLE distribution[42] and on the Internet.[63] For the absolute vertical excitation energies we find that the more diffuse $\pi-\pi^*$ excitation shows a strong basis set dependence (see Table 2). The additional flexibility of

Table 2. Basis Set Dependence of the Calculated ADC(2) Vertical Excitation Energies ΔE and Solvent Shifts Δ_{sol} for the Acrolein Molecule[a]

	$(n-\pi^*)$			$(\pi-\pi^*)$		
	$\Delta E_{I,0}^{\mathrm{vac}}$	$\Delta\mathcal{G}_{I,0(\mathrm{eq})}$	Δ_{sol}	$\Delta E_{I,0}^{\mathrm{vac}}$	$\Delta\mathcal{G}_{I,0(\mathrm{eq})}$	Δ_{sol}
SVP	3.75	3.87	0.12	7.11	6.66	−0.45
TZVP	3.72	3.85	0.14	6.90	6.41	−0.49
TZVPP	3.69	3.84	0.15	6.79	6.33	−0.46
QZVPP	3.69	3.85	0.16	6.71	6.25	−0.46

[a]All values are in electronvolts. COSMO parameters are $\varepsilon = 40.0$ and $n = 1.5$. The MP2/TZVPP in vacuo structure was used throughout.

the s and p set (as probed by moving from SVP to TZVP) is important for a qualitatively correct picture, additional polarization functions (TZVP to TZVPP and TZVPP to QZVPP) help to better describe differential correlation. We note the usual rule of thumb that for basis sets of TZVPP quality, the basis set truncation error and the correlation error (error in comparison to more involved method) are of the same size.[64] This means that larger basis sets do, on average, not improve the accuracy of MP2 or ADC(2) results.

Despite the substantial differences for absolute excitation energies, the solvent shifts are nearly unaltered. For the $n-\pi^*$ transition, we find a weak basis set dependence for both excitation energies and solvent shifts.

The procedure to construct the cavity around the molecule is, unfortunately, by no means uniquely determined.[10,15] Here, we use the standard COSMO cavity construction scheme as described in ref 15 resulting in a cavity which is of SAS (solvent accessible surface) type. It is controlled by a set of parameters, atomic radii (the relevant radii for acrolein, used in this work, are $r_C = 2.00$ Å, $r_O = 1.72$ Å, $r_H = 1.30$ Å) and a solvent radius $r_{\mathrm{solv}} = 1.30$ Å. These parameters were optimized for treating ground state solvation effects (actually within an extended scheme that uses COSMO calculations as basic ingredient).[65] Using the same parameters for excited state solvation energies is hence only an ad hoc solution, and one has to worry about the effect of modifying these.

Here, we exemplarily study the influence of a uniform scaling of the atomic radii on the excitation energies, the transition moments and excited state dipole moments (r_{solv} is kept constant). In Figure 2, we report the results for scaling factors

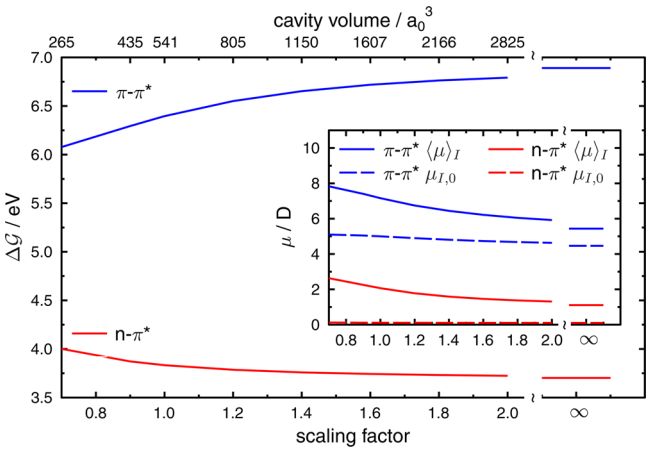

Figure 2. Vertical free excitation energies $\Delta\mathcal{G}_{I,0(\mathrm{eq})}$, transition dipole moments $\mu_{I,0}$ and static excited state dipole moments $\langle\mu\rangle_I$ for the acrolein molecule calculated at the ADC(2)/TZVP level using $\varepsilon = 40$, $n = 1.5$ for the solvent model. All energy contributions described in the theory part of this work are included in these calculations. The standard radii for constructing the cavity are scaled by a factor to show the dependence of energies and properties on the cavity size (the respective cavity volume is reported on the upper ordinate). For comparison, corresponding vacuum values of the properties are shown at the right of each graph.

between 0.7 and 2.0, the physically meaningful range is between 0.9 and 1.2. It is interesting to observe, however, that for a scaling factor of 2.0 all values are basically converged to those of the isolated molecule.

Due to its smaller excited state dipole moment (and vanishing transition dipole moment), the $n-\pi^*$ transition is less dependent on the scaling factor than the $\pi-\pi^*$ transition is. The changes in the $n-\pi^*$ excitation energy are +0.04 and −0.05 eV for the scaling factors 0.9 and 1.2, respectively; for the $\pi-\pi^*$ excitation, the changes are −0.10 and +0.16 eV. The transition dipoles are rather independent of the uniform scaling, whereas the excite state dipole moment increases significantly if the cavity volume shrinks; see Figure 2. This is not unexpected as a smaller distance between the molecule and the cavity surface enhances the (stabilizing) interactions of the solute with the surface charges. This promotes the redistribution of solute charges in order to create higher electrostatic moments on the solute.

The lesson to learn from this simple scaling example is the following: The results from continuum solvation models of the present level of sophistication are sufficiently stable (with respect to the choice of parameters) to give results with semiquantitative accuracy, i.e. if errors of the order of 0.2 eV are not an issue. Note that the accuracy of the underlying theory, ADC(2), is not better than that in general. More elaborate models might construct the cavity based on the isodensity.[66]

4.1.3. Comparison to Experiment and Other Approaches. The solvent shift from vacuum to aqueous solution has been

dx.doi.org/10.1021/ct300763v | J. Chem. Theory Comput. 2013, 9, 977−994

discussed in several previous publications;[6,29,31] in particular there exist recent experimental results.[62] In Table 3, we have collected the ADC(2)/COSMO predictions for the $n-\pi^*$ and $\pi-\pi^*$ transition, together with experimental and other recent theoretical results.

Table 3. Calculated Solvent Shifts Δ_{sol} (eV) for Acrolein in Comparison to Experiment and Other Work[a]

	$(n-\pi^*)$			$(\pi-\pi^*)$		
	$\Delta E^{vac}_{1,0}$	$\Delta \mathcal{G}_{1,0(eq)}$	Δ_{sol}	$\Delta E^{vac}_{2,0}$	$\Delta \mathcal{G}_{2,0(eq)}$	Δ_{sol}
ADC(2), (no LR)[b]	3.69	3.86	+0.17	6.79	6.57	−0.21
ADC(2)[b]	3.69	3.86	+0.17	6.79	6.40	−0.39
ADC(2), RF(SCF)[b,c]	3.69	3.86	+0.18	6.79	6.31	−0.48
ADC(2)[d]	3.69	3.81	+0.13	6.79	6.37	−0.42
ADC(2), $+H_2O$[b,e]	3.69	4.17	+0.48	6.79	6.27	−0.52
exp[f]	3.69	3.94	+0.25	6.41	5.90	−0.51
CCSDR(3)/MM[g]	3.81	4.08	+0.27	6.73	6.22	−0.51
CCSD/PCM[h]	3.94	4.14	+0.20	6.89	6.54	−0.35
SAC-CI/PCM[i]	3.85	3.95	+0.10	6.97	6.75	−0.22

[a]Calculations at the ADC(2)/TZVPP level of theory, using $\varepsilon = 78.4$, $n = 1.33$ as parameters for the solvation model. [b]Using the in vacuo MP2/TZVPP structures. [c]Using the SCF reaction field of the ground-state. [d]Using reoptimized ground-state structures including solvent effects (MP2/TZVPP, PTE-formalism). [e]Including one explicit water molecule. [f]Reference 62. [g]Reference 6. [h]Reference 29. [i]Reference 31, cc-pVTZ basis.

As detailed in section 4.1.1, the inclusion of linear response terms does not influence the predicted solvent shift of the $n-\pi^*$ transition, but for the $\pi-\pi^*$ transition the shift is nearly doubled (see the first two lines in Table 3). With that, we obtain results which are in fair agreement with experimental findings, a slight upshift of the $n-\pi^*$ transition (+0.17 eV vs the experimental value of +0.25 eV) and a strong downshift for the $\pi-\pi^*$ transition (−0.39 eV vs the experimental value of −0.51 eV). It should be kept in mind, however, that we used a very simplistic theoretical model that relies on vertical excitations only, using a single in vacuo structure for acrolein. We also recall the dependence on the choice of cavity parameters, as reported in section 4.1.2

In addition, we have checked the following approximation. As noted above, the calculation of a self-consistent reaction field for the ground state leads to a large increase in computation time. Hence we have tested the effect of using the reaction field from the Hartree−Fock reference state. This results in a tiny effect for the $n-\pi^*$ transition, the $\pi-\pi^*$ transition is further downshifted by a little more than −0.1 eV. But still, the qualitative picture holds. Also, the effect of using a different structure for the ground state is small. Instead of the in vacuo structure, we use a structure optimized at the MP2/COSMO level (in the PTE formalism),[60] leading to a change of −0.05 eV for both the $n-\pi^*$ and the $\pi-\pi^*$ transition.

On the other hand, water as solvent is a rather problematic case as far as continuum solvation models are concerned, due to its capability to form hydrogen bonds. To examine the effect, we add one explicit water molecule in the quantum-chemical treatment (as indicated in Scheme 1, **1a**). Indeed, this has a strong effect on both transitions, the $n-\pi^*$ transition is shifted to higher energies by another 0.31 eV, and the $\pi-\pi^*$ transition is shifted down, now fortuitously agreeing with the experimental outcome. Certainly, a more realistic account for hydrogen bond effects requires a proper statistical average over possible interaction geometries. Nevertheless the result indicates that the effect must be taken into account in order to arrive at a quantitatively correct prediction of the solvent shift.

A good agreement with experiment was reported by Sneskov et al.[6] who used an explicit QM/MM solvation model in combination with a highly accurate quantum chemical treatment of the solvate. The solvent shifts and the absolute absorption maxima were reproduced within 0.02 eV. We note that a comparison of the in vacuo excitation energies of ADC(2) and CCSDR(3) indicates a surprisingly good accuracy for the much simpler second-order method. This is in accord with the observation that typically second-order methods give a rather good average accuracy which usually is only improved at a coupled-cluster level *beyond* CCSD, i.e. with perturbative inclusion of connected triples clusters.[64]

Compared to ADC(2)/COSMO, the CCSD/PCM calculations of Caricato et al.[29] seem to give better predictions for the $n-\pi^*$ solvent shifts, but they perform slightly worse for the $\pi-\pi^*$ transition. The origin of this difference is difficult to isolate, as both the underlying electronic structure method and the solvation treatment differ (the authors of ref 29 use a self-consistent procedure for the nonequilibrium corrections). In general we can expect that the differences between the solvation models themselves, i.e. PCM and COSMO, should be not significant. This is indicated by a comparison to SAC-CI/PCM calculations[31] which result in solvent shifts very similar to ADC(2)/COSMO if the response terms are omitted (which seems to be the case in the derivation of the SAC-CI/PCM formalism[31]).

4.2. Ethene Dimer. The ethene dimer, **2**, is employed as a toy system to investigate excitonic coupling in the excited state. A similar study can also be found in the work of Iozzi et al.[49] who calculated the excitonic coupling by a fragment approach within the TDDFT framework.

In the following, we need to formally distinguish the two monomers of the system, we will call them A and B for simplicity and associate them with states $|\Psi_A\rangle$ and $|\Psi_B\rangle$. Then, we assume a wave function $|\Psi_{A^*B}\rangle$ that describes the unperturbed system in which molecule A is in its excited electronic state and B is in its ground electronic state, and vice versa for $|\Psi_{AB^*}\rangle$. In terms of these states, the coupling is

$$V_{AB} = \langle \Psi_{A^*B} | \hat{H} | \Psi_{AB^*} \rangle \tag{68}$$

$$\approx \int \mathrm{d}^3\mathbf{r}_1\, \mathrm{d}^3\mathbf{r}_2\, \gamma^A_{0f}(\mathbf{r}_1) \frac{1}{|\mathbf{r}_1 - \mathbf{r}_2|} \gamma^B_{0f}(r_2)$$

$$(\text{for } |\Psi_{A^*B}\rangle \rightarrow |\Psi_{A^*}\Psi_B\rangle, \text{ etc.}) \tag{69}$$

$$\approx \frac{\boldsymbol{\mu}^A_{0f} \cdot \boldsymbol{\mu}^B_{0f}}{R_{AB}{}^3} - 3\frac{(\boldsymbol{\mu}^A_{0f} \cdot \mathbf{R}_{AB})(\boldsymbol{\mu}^B_{0f} \cdot \mathbf{R}_{AB})}{R_{AB}{}^5} \qquad (\text{for } R_{AB} \rightarrow \infty) \tag{70}$$

Under certain conditions, as indicated, the coupling term can be expressed in terms of monomer quantities. If the total wave function is well represented by the antisymmetrized product of the (unperturbed) monomer wave functions, $|\Psi_{A^*B}\rangle \approx |\Psi_{A^*}\Psi_B\rangle$ and $|\Psi_{AB^*}\rangle \approx |\Psi_A\Psi_{B^*}\rangle$, V_{AB} may be expressed as a Coulomb integral involving the transition densities $\gamma^A_{0f}(\mathbf{r})$ and $\gamma^B_{0f}(\mathbf{r})$, defined as, e.g., $\gamma^A_{0f}(\mathbf{r}) = \Psi_A(\mathbf{r})\Psi^*_{A^*}(\mathbf{r})$. For large separations R_{AB}

dx.doi.org/10.1021/ct300763v | J. Chem. Theory Comput. 2013, 9, 977−994

this integral can be further approximated by the leading order terms of its multipole expansion, a dipolar coupling involving the transition dipole moments $\boldsymbol{\mu}_{0f}^{A}$ and $\boldsymbol{\mu}_{0f}^{B}$ of the monomers (e.g., $\boldsymbol{\mu}_{0f}^{A} = \langle \Psi_A | \hat{\boldsymbol{\mu}} | \Psi_{A^*} \rangle$).

When solving the electronic Schrödinger equation for the coupled dimer, we obtain the adiabatic wave functions and energies, and the coupling gives rise to a splitting $\Delta\Omega = 2V_{AB}$ of the initially (i.e., for the uncoupled system) degenerate electronic states $|\Psi_{A^*B}\rangle$ and $|\Psi_{AB^*}\rangle$. This level splitting is often called Davydov splitting, a term originally devised for the corresponding band splitting in molecular crystals.[67] In the present work, we use this approach to calculate V_{AB} (supermolecular approach). We note that for sufficiently separated chromophores, the approach based on the transition densities of the fragments, eq 69, is more efficient (as used, for instance, in the work of Iozzi et al.[49]). For close or chemically linked dimers, the supermolecular approach is more reliable, however.

In the presence of a surrounding medium, two effects occur.[49] First, the monomeric wave functions are altered, leading to a solvent shift and a change of the transition densities. For the ideal dimer the energy shift is the same at both sites and hence has no influence on the splitting. The change in the transition density, however, will typically result in an enhancement of the transition dipole moments and consequently in an enhancement of the resonance interaction; eq 68. On the other hand, the polarizable medium will screen the interaction of the transition moments which again reduces the interaction.

Both effects are accounted for by a polarizable continuum approach, as first outlined by Iozzi et al.[49] This requires, however, the presence of the linear response terms, as we will show below numerically. In total, we will observe an effective screening of the coupling

$$s_{\text{eff}} = \frac{V_{AB,\text{sol}}}{V_{AB,\text{vac}}} \tag{71}$$

This may be compared with more approximate treatments of the solvent effects, as for example in Förster's theory of resonance energy transfer (FRET).[68] Here, the screening is accounted for by a factor of

$$s_F = \frac{1}{n^2} \tag{72}$$

which stems from a modification of the Coulomb interaction in eq 68. The effect of the intervening medium is accounted by including its dielectric constant at high frequency, approximated by the square of the refractive index n: $1/r \rightarrow 1/(\varepsilon(\omega)r) \approx 1/(n^2 r)$. A closer analysis, however, shows that this choice is not really consistent with dipolar interactions.[69] As, for example, worked out by Onsager,[18] the external field of a dipole (hosted in a spherical cavity) is screened by

$$s_O = \frac{3}{2n^2 + 1} \tag{73}$$

We have obtained $\Delta\Omega = \mathcal{G}_{2,0(\text{eq})} - \mathcal{G}_{1,0(\text{eq})}$ for the ethene dimer at several distances R_{AB} by calculating the adiabatic energies of the supermolecular system. The slow part of the reaction field is determined for the ground state, that is Hartree–Fock SCF for CIS and MP2 for ADC(2). The results are shown in Figure 3. One immediately notices that the expected screening effects are only present, if we include the linear response terms.

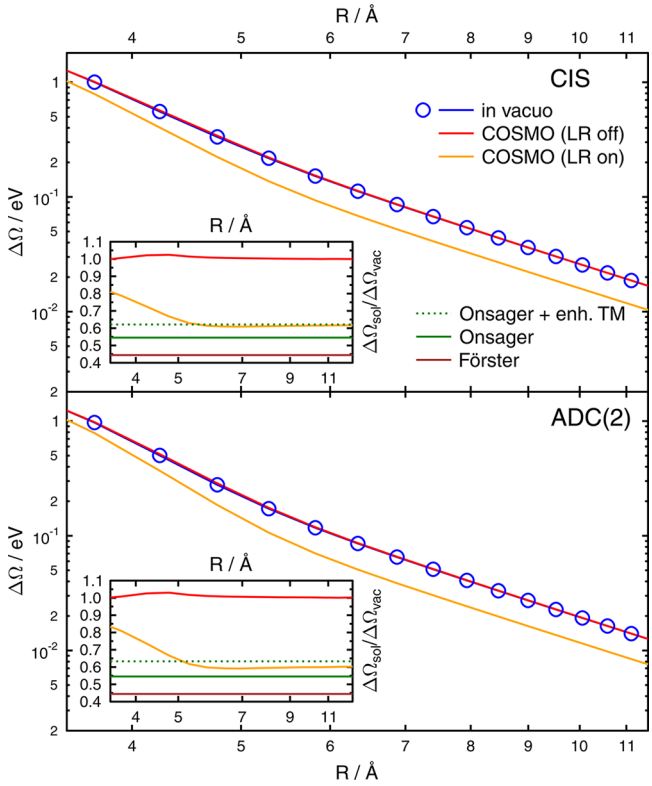

Figure 3. Ethene dimer: calculated distance dependence of the Davydov splitting in vacuo and for solvated molecules (ε = 40.0, n = 1.5). Results are shown for CIS (upper graph) and ADC(2) (lower graph). The TZVP basis set was used. The screening effect of the solvent is reproduced only when the linear response terms (LR) are included. The inset shows the effective screening factor and compares to the constant screening factors used in Förster theory ($1/n^2$) and Onsager theory ($3/(2n^2 + 1)$). The dashed line is based on the Onsager model, too, but includes a correction for the enhanced transition moment in solution (from monomer calculation). ADC(2) does not cleanly separate into contributions from well-defined monomer transition dipoles, hence the slightly larger deviation from the dashed line (see text).

For distances beyond 6 Å, the effective screening s_{eff} tends to a constant, but at shorter distances it changes significantly (note that the cavities are joined for R_{AB} < 5.3 Å). For all R_{AB}, the screening factor is closer to unity than the one used in Förster theory, but for large separations it compares well with the Onsager screening factor, once we also account for the increase of the monomer transition dipole moment due to the solvent. This factor can be obtained by calculating the transition moment of the monomer in vacuo and in the presence of the COSMO reaction field.

For CIS, we find at distances >8 Å a nearly perfect agreement of COSMO and the Onsager screening factor. This reassures us that the surface charges of COSMO lead to a physically consistent screening of the long-range Coulomb interactions. For ADC(2), we get a slight deviation of s_{eff} and s_O in the long-range limit. This is mainly because the long-range behavior of the ADC(2) eigenvalue problem, eq 50, does not reproduce an interaction that is proportional to the square of ADC(2) transition densities, as defined in ref 53. This is due to the strict

truncation of terms at second-order, as outlined in section 3.4 (cf. the explicit expressions for the ADC(2) energy expressions, Table 1).

4.3. Perylene-tetracarboxy-diimide Dimer. The *N*,*N*-linked dimer of perylene-tetracarboxy-diimide (PTCDI) has been previously studied by single-molecule spectroscopy and serves as a model system for energy transfer.[70] In these experiments, the molecules are embedded in a rigid matrix of poly(methyl metacrylate) (PMMA), which makes it necessary to model the effective screening by the environment. Using $s_F = 1/n^2$ seems to give a too strong screening and does not account for the short distance between the two chromophores.

For the present study, we use the MP2/SVP optimized in vacuo structure of the ground state and calculate the two lowest excited singlet states at the ADC(2)/SVP level of theory. The COSMO solvation model is applied with $n = 1.49$ and $\varepsilon = 2.2$. The low value for ε accounts for the limited flexibility of the nuclear degrees of freedom in a polymer matrix. The choice of ε, however, is not important for the splitting in the present case. As for the previous example, we find that only the linear response terms contribute to the screening. The other terms of the solvation treatment have an effect on the total excitation energies but do not influence the splitting.

The static reaction field turns out to be unimportant for the calculation of the screened splitting, even with the Hartree–Fock reaction field (effectively avoiding any costly solvent iteration) we obtain the same result as for the fully self-consistent reaction field. This outcome is not unexpected as the molecule, also the monomer units, are not dipolar. The effective screening is 0.69 (see Table 4) which is a larger value than predicted with $1/n^2 = 0.45$ and $3/(2n^2 + 1) = 0.55$.

Table 4. Calculated Davydov Splitting ΔΩ (eV) between the 1^1B_1 and 1^1A excited state of the PTCDI Dimer[a]

reaction field	LR term	$\Delta\mathcal{G}_{1,0}$/eV	$\Delta\mathcal{G}_{2,0}$/eV	ΔΩ/eV	s_{eff}[b]
in vacuo		2.641	2.747	0.106	
S_0(HF)	neglected	2.546	2.654	0.109	1.024
S_0(MP2)	neglected	2.631	2.739	0.108	1.019
S_0(HF)	included	2.456	2.529	0.073	0.689
S_0(MP2)	included	2.541	2.613	0.073	0.685

[a]All calculations are carried out at the ADC(2)/SVP level. Given are the excitation energies ΔE and the splitting ΔΩ, with the linear-response (LR) terms switched on or off in the calculations of the excitation energies. In addition, we test the effect of using either the reaction field from the Hartree–Fock density or the one self-consistently obtained from the MP2 density. The solvent parameters are $n = 1.49$ and $\varepsilon = 2.2$. [b]Effective screening factor, $s_{eff} = \Delta\Omega_{solv}/\Delta\Omega_{vac}$. For comparison, $s_F = 1/n^2 \approx 0.450$.

4.4. Intramolecular Charge Transfer: 4-(*N*,*N*-Dimethylamino)benzonitrile (DMABN). As a further example application of the ADC(2)/COSMO implementation, we will here extend our earlier study of DMABN, originally carried out at the CC2 level and not accounting for environment effects.[71] 4-(*N*,*N*-Dimethyl-amino)-benzonitrile (DMABN) is a model compound for dual fluorescence, that is under certain conditions emission from two different electronic states is observed.[72,73] One of these gives rise to a "normal" emission band with a small Stokes shift as expected for this class of compounds. In the literature, the emitting state is usually called locally excited (LE) state. The other electronic state can be characterized as an intramolecular charge-transfer (ICT) state and gives rise to a strongly red-shifted emission with a strong solvent dependence. DMABN and related compounds were studied extensively over the last decades.[71,74−84]

In the following, we will use the CC2/TZVPP in vacuo structures from ref 71 which were optimized for the S_0, the S_1(LE), and the S_1(ICT) state and check for solvent effects by carrying out single-point ADC(2)/TZVPP calculations with COSMO. The reaction field is in all cases obtained self-consistently for the respective state for which the structure was optimized, that is the S_0 state (treated at the MP2/TZVPP level of theory) in case of the ground state structure and for the S_1 state in the other cases. The vertical energy separations to the other states were corrected for the fast response part of the reaction field, eq 59.

In ref 71, it was found that the ICT state of the isolated molecule does not have C_{2v} symmetry (with the amino-group twisted by 90°); rather, this structure (called ICT-S in the following) turned out to be a saddle point on the S_1 energy surface . The energy is further lowered if in addition a pyramidalization of the C_4 atom is allowed for, leading to an out-of-plane bending of the amino-group, as confirmed by other studies[78,82] (this structure will be denoted ICT-D in the following). This distortion, however, also leads to a significant lowering of the dipole moment and it was therefore conjectured that the C_{2v} structure will become a minimum in sufficiently polar solvents.[71]

The results of the ADC(2) calculations are collected in Figure 4. For the gas phase, ADC(2) reproduces all the features of the energy ordering seen for CC2 in ref 71. The LE state is the lowest excited state for vertical excitations, i.e. at the ground state (GS) structure, and its energy is slightly lowered if the structure is optimized for that state. LE and ICT state interchange their energetic sequence upon twisting of the amino-group, and for both structures, ICT-S and ICT-D, the ICT state is the lowest state. It carries, in particular for the ICT-S structure, a strong dipole moment of 15 D. As pointed out in ref 71, the relative ordering of the energetic minima of the LE and the ICT state is not correct at the second-order level of theory (as seen in Figure 4, the ICT minimum is below the LE minimum by 0.1 eV). Experiments show that DMABN is not dually fluorescent in the gas phase and in nonpolar solvents. In fact, single-point calculations with a higher-order CC method, CCSDR(3), indicate that the ICT level should be shifted to higher energy by approximately 0.2 eV relative to the LE level.[71]

For studying solvent effects, we choose two parameter sets: One that represents an unpolar solvent ($\varepsilon = 1.9$, $n = 1.37$ corresponding to *n*-hexane) and one that is typical for a polar solvent ($\varepsilon = 37.5$, $n = 1.34$ corresponding to acetonitrile). A self-consistent reaction field was calculated for the electronic state corresponding to the respective minimum structure (i.e., the S_0 reaction field at the GS structure and the S_1 reaction field at each of the other structures), and the energies of the other states were obtained using the nonequilibrium formalism, eq 59.

For the unpolar solvent, we do not find any significant changes of the relative energy levels; see Figure 4b. In comparison to the gas phase results, the dipole moments are generally enhanced by 1−2 D. The S_1 energy difference between two ICT structures becomes smaller; relative to the S_1(LE) minimum, they are energetically favored by a little more than 0.2 eV. The energy correction from higher-order CC

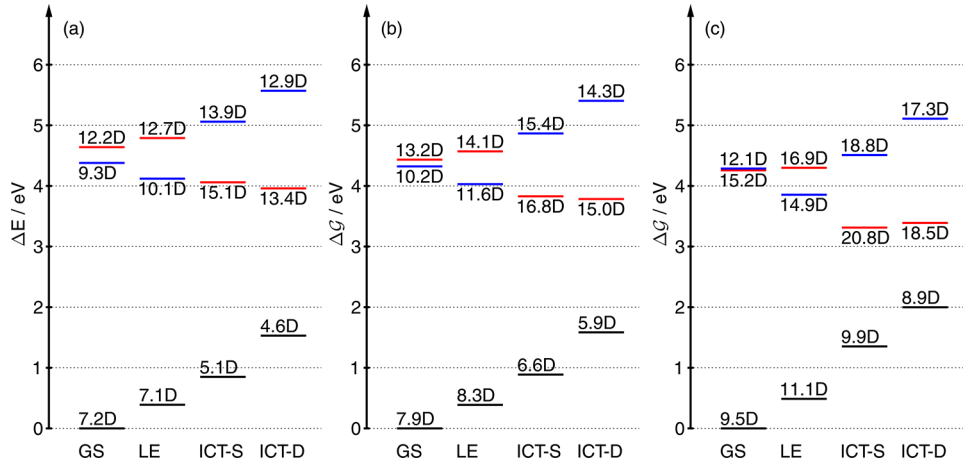

Figure 4. Energy levels of DMABN in different environments: (a) gas phase, (b) *n*-hexane (ε = 1.9, n = 1.37), and (c) acetonitrile (ε = 37.5, n = 1.34) calculated at the ADC(2)/TZVPP level. The geometries of the isolated molecules have been optimized at the CC2/TZVPP level for different states as indicated. GS stands for ground state, LE for locally excited state, and ICT for intramolecular charge transfer state, where ICT-S is the C_{2v} symmetric structure (first-order saddle point in the calculations for the isolate molecule) and ICT-D is the distorted structure (the minimum in the calculations for the isolated molecule). The structures where taken from ref 71. The energies are given in electronvolts relative to the ground state minimum. Color code: black = GS, blue = LE, red = ICT. For every state the expectation value of the dipole moment is given in Debye units.

methods (+0.2 eV, see above), however, suggests that LE and ICT minima are on the same energetic level and the thermal equilibration of the two states is inhibited by a small barrier between them (not considered here, barriers for a related system were discussed in ref 77). Hence, the results are still in concert with the experimental finding that no visible ICT emission is observed for DMABN in *n*-hexane.

For strongly polar solvents, a significant downshift of the S_1(ICT) energies is predicted; see Figure 4c. The dipole moments are even more strongly enhanced, as compared with the results for the gas-phase and for the apolar solvent. The energy at the symmetric ICT-S structure is now indeed below the energy at the ICT-D structure, as conjectured above. In contrast to that the LE state is shifted very little, in accord with experimental measurements of the solvatochromic shifts of LE and ICT emission.[85]

The experimental solvent shift from *n*-hexane to acetonitrile is 0.19 eV for the $S_2 \leftarrow S_0$ absorption maximum (calculated 0.15 eV), 0.25 eV for the LE emission maximum (calculated 0.28 eV), and 0.92 eV for the ICT emission (calculated 0.98 eV). The last experimental number originates from an extrapolation, as for unpolar solvents like *n*-hexane the ICT emission is not observed. The calculation assumes that the ICT-S structure is relevant for the emission process. The values for the dipole moments and the solvent shifts are also in good agreement with other computational studies on DMABN that include solvent effects, e.g. ref 82.

The results for DMABN let us expect that the present implementation can successfully augment future studies on the photophysical properties of similar molecular systems. In particular, it helps to more accurately bridge the gap between predictions for isolated molecules and experimental measurements in solution.

5. CONCLUSIONS

We have derived and implemented a model to treat solvent effects for electronically excited molecules within the ADC(2) method, based on the conductor-like screening model (COSMO). The model takes care of two types of solvent effects:

One effect is due to the interaction of the permanent charge distribution of the molecule with the reaction field in the surrounding polarizable medium induced by this charge distribution. This effect is recovered in state-specific approaches, which explicitly take into account the electron densities of the respective states. If the state is long-lived (the ground state or the lowest excited singlet or triplet state), the molecules in the environment can fully relax toward the new charge distribution, which in terms of the COSMO model means that the reaction field and the density should be obtained self-consistently. Energy differences to short-lived states require a special treatment, as only the fast part of the reaction field (corresponding to the purely electronic polarizability of the environment) will be able to relax. For these states, we adopt the perturbative correction scheme of Caricato et al.[26]

The second solvent effect corresponds to an excitonic coupling of the solute and solvent molecules (a coupling of the transition density of the solute and the dynamic response of the reaction field). This leads to an enhancement of transition dipole moments in solution and to the screening of excitonic couplings between excitations that are localized on spatially separated chromophores. Terms describing this type of solvent effect result from a linear-response treatment of the system, and they consist of a coupling of the transition density and the corresponding response of the fast part of the reaction field. Such contributions are needed for calculating the excitation energy transfer couplings in condensed phase, as proposed by Iozzi et al.[49] for TDDFT and the PCM solvation model (their model does not include state-specific corrections, however). On the other hand, it was argued, for example in ref 43, that the linear response terms should be regarded as dispersion terms, which are beyond a purely electrostatic solvation model. Therefore these terms were dropped in favor of the state-specific correction terms.

Here, we argue that both contributions are equally important, as they describe linearly independent physical effects. Therefore, both types of terms are included in our ADC(2)/COSMO implementation. The implementation is based on the RICC2 module of TURBOMOLE. At present, only single point

calculations are supported, the self-consistent reaction field is obtained by a macro-iteration procedure.

We have presented a number of sample applications that illustrate the use of the present ADC(2)/COSMO implementation. The examples also support our analysis that both state-specific and linear-response terms should be accounted for. While, compared with a purely state-specific scheme, solvent shifts on vertical excitations are not spoiled by additionally including the linear response contributions (the results even indicate a slight improvement for solvent shift of transitions with a strong transition dipole), the inclusion of linear response contributions turns out to be indispensable when excitonic couplings are investigated.

We finally note that the formalism for apparent surface charge models is very similar to models that use an embedding in polarizable force fields[7,8] which gives perspective to transferring the present implementation to atomistic embedding models.

A. DERIVATION OF EQUATIONS 17 AND 24

We briefly describe the derivation of the response equations, in particular the structure of the free energy matrix $G^{[2]}_{xy}$, eqs 17 and 24. We follow the formalism as described in refs 46, 47, and 43 and generalize to the case that the ground state $|\Psi_0\rangle$ (acting as the reference state for the response formalism) and the state that is in equilibrium with the solvent $|\Psi_{I(\mathrm{eq})}\rangle$ are not the same.

We start by defining a free energy operator

$$\begin{aligned}\hat{G}(t) = \hat{H} &+ \frac{1}{2}\hat{\mathbf{V}}\cdot\langle\Psi_0(t)|\hat{\mathbf{Q}}^{\mathrm{f}}|\Psi_0(t)\rangle \\ &+ \hat{\mathbf{V}}\cdot\langle\Psi_{I(\mathrm{eq})}|\hat{\mathbf{Q}}^{\mathrm{s}}|\Psi_{I(\mathrm{eq})}\rangle \\ -\frac{1}{2}&\langle\Psi_{I(\mathrm{eq})}|\hat{\mathbf{V}}|\Psi_{I(\mathrm{eq})}\rangle\cdot\langle\Psi_{I(\mathrm{eq})}|\hat{\mathbf{Q}}^{\mathrm{s}}|\Psi_{I(\mathrm{eq})}\rangle + \hat{X}(t)\end{aligned} \tag{74}$$

which contains an arbitrary time-dependent perturbation. For the sake of this derivation, it is sufficient to consider a periodic perturbation that has been switched on adiabatically slow and which vanishes for $t \to -\infty$.[46] The operator has been constructed such that for vanishing $\hat{X}(t)$ its expectation value $\langle\Psi_0|\hat{G}|\Psi_0\rangle$ recovers eq 5 for $I = 0$ and eq 8 otherwise.

The time-dependent ground state $|\Psi_0(t)\rangle$ is parametrized as given in eq 14. In order to obtain equations of motion for the parameters $s_n(t)$, the Frenkel variational principle is employed. This leads to a set of equations, which can be recast into a form known as generalized Ehrenfest equations:[46]

$$\begin{aligned} i\,&\frac{\mathrm{d}}{\mathrm{d}t}\langle\Psi_0(t)|\tilde{\hat{\tau}}_x^{\dagger}|\Psi_0(t)\rangle \\ &= \langle\Psi_0(t)|\frac{\partial\tilde{\hat{\tau}}_x^{\dagger}}{\partial t}|\Psi_0(t)\rangle + i\langle\Psi_0(t)|[\tilde{\hat{\tau}}_x^{\dagger}, \hat{G}]|\Psi_0(t)\rangle \\ &\quad + i\frac{1}{2}\langle\Psi_0(t)|[\tilde{\hat{\tau}}_x^{\dagger}, \hat{Q}^{\mathrm{f}}]|\Psi_0(t)\rangle\langle\Psi_0(t)|\hat{V}|\Psi_0(t)\rangle \end{aligned} \tag{75}$$

Here, we used transformed operators

$$\tilde{\hat{O}} = \mathrm{e}^{-i\hat{S}(t)}\hat{O}\mathrm{e}^{i\hat{S}(t)} \tag{76}$$

The last term of the right-hand side stems from the $|\Psi_0(t)\rangle$-dependent term of $\hat{G}(t)$; see eq 74. There is also an adjoint set of equations (for $\tilde{\hat{\tau}}_x$). For the parametrization chosen here, the two sets of equations decouple. We also note that the left-hand side of eq 75 was only added for clarity, for the special case of transfer operators it vanishes and the equations of motion are only determined by the right-hand side.

The first term of the right-hand side can be expanded up to second-order in the perturbing operator $\hat{X}(t)$, as follows:

$$\langle\Psi_0(t)|\frac{\partial\tilde{\hat{\tau}}_x^{\dagger}}{\partial t}|\Psi_0(t)\rangle = i\sum_y\langle\Psi_0|[\tau_x^{\dagger}, \hat{\tau}_y]|\Psi_0\rangle\dot{s}_y + \ldots \tag{77}$$

$$= i\sum_y S^{[2]}_{xy}\dot{s}_y + \ldots \tag{78}$$

The other terms lead to (again up to second-order):

$$\begin{aligned} &i\langle\Psi_0(t)|[\tilde{\hat{\tau}}_x^{\dagger}, \hat{H} + \hat{X}(t)]\rangle + i(\langle\Psi_{I(\mathrm{eq})}|[\tilde{\hat{\tau}}_x^{\dagger}, \hat{\mathbf{Q}}^{\mathrm{s}}]|\Psi_{I(\mathrm{eq})}\rangle \\ &\quad + \langle\Psi_0(t)|[\tilde{\hat{\tau}}_x^{\dagger}, \hat{\mathbf{Q}}^{\mathrm{f}}]|\Psi_0(t)\rangle)\langle\Psi_0(t)|\hat{\mathbf{V}}|\Psi_0(t)\rangle \\ &= i\langle\Psi_0|[\tilde{\hat{\tau}}_x^{\dagger}, \hat{X}(t)]|\Psi_0\rangle - \sum_y\langle\Psi_0|[\tilde{\hat{\tau}}_x^{\dagger}, [\hat{H}, \tau_y]]|\Psi_0\rangle s_y \\ &\quad - \sum_y\langle\Psi_0|[\tilde{\hat{\tau}}_x^{\dagger}, [\hat{\mathbf{V}}, \tau_y]]|\Psi_0\rangle(\langle\Psi_{I(\mathrm{eq})}|\hat{\mathbf{Q}}^{\mathrm{s}}|\Psi_{I(\mathrm{eq})}\rangle \\ &\quad + \langle\Psi_0|\hat{\mathbf{Q}}^{\mathrm{f}}|\Psi_0\rangle)s_y - \sum_y\langle\Psi_0|[\tilde{\hat{\tau}}_x^{\dagger}, \hat{\mathbf{V}}]|\Psi_0\rangle \\ &\quad \langle\Psi_0|[\hat{\mathbf{Q}}^{\mathrm{f}}, \hat{\tau}_y]|\Psi_0\rangle s_y + \ldots \end{aligned} \tag{79}$$

$$= iX^{[1]}_x(t) - \sum_y E^{[2]}_{xy}s_y(t) - \sum_y \mathbf{V}^{[2]}_{xy}(\mathbf{Q}^{\mathrm{s}}_{I(\mathrm{eq})} + \mathbf{Q}^{\mathrm{f}}_0)s_y(t) - \sum_y \mathbf{V}^{[1]}_m\mathbf{Q}^{[1]}_n s_y(t) + \ldots \tag{80}$$

$$= iX^{[1]}_x(t) - \sum_y G^{[2]}_{xy}s_y(t) + \ldots \tag{81}$$

The equation of motion to second-order thus takes the form

$$\sum_y iS^{[2]}_{xy}\dot{s}_y(t) - \sum_y G^{[2]}_{xy}s_y(t) = -iX^{[1]}_x(t) \tag{82}$$

By a Fourier transformation, we obtain the equations for the frequency components of the perturbation $\hat{X}(\omega)$. The response vectors $s_y(\omega)$ can be used to determine the linear response function of the system.[46,47] This response function has a pole structure, and the poles are the eigenvalues of eq 16, which thus is the main working equation for determining excited states in the linear response formalism. Equation 24 can be identified from eqs 79−81, and eq 17 follows from eq 24 for $I = 0$.

B. ADC(2) EXCITED STATE ONE-PARTICLE DENSITIES

We start from the following Lagrange functional for the ADC(2) energy[34]

$$\begin{aligned} L = &\langle 0|\hat{H}|0\rangle + \langle 0|\hat{H}_N\hat{T}_2|0\rangle \\ &+ \langle 0|\hat{R}_1^{\dagger}\left[\hat{H}_N + \frac{1}{2}[\hat{H}_N, \hat{T}_2] + \frac{1}{2}[\hat{T}_2^{\dagger}, \hat{H}_N], \hat{R}_1\right]|0\rangle \\ &+ \langle 0|\hat{R}_1^{\dagger}\hat{H}_N\hat{R}_2|0\rangle + \langle 0|\hat{R}_2^{\dagger}\hat{H}_N\hat{R}_1|0\rangle + \langle 0|\hat{R}_2^{\dagger}\hat{F}_N\hat{R}_2|0\rangle \\ &+ \omega(1 - \langle 0|\hat{R}^{\dagger}\hat{R}|0\rangle) + \langle 0|\hat{N}_2(\hat{H}_N + \hat{F}_N\hat{T}_2)|0\rangle \\ &+ \langle 0|\hat{Z}\hat{F}_N|0\rangle \end{aligned} \tag{83}$$

dx.doi.org/10.1021/ct300763v | J. Chem. Theory Comput. 2013, 9, 977−994

where the first two terms are the reference energy (E_0) and the MP2 correlation energy, followed by the expression for the ADC(2) excitation energy; cf. Table 1. The Lagrange multiplier ω is associated with the normalization condition, whereas the amplitudes n_{ij}^{ab} in the operator $\hat{N}_2$ are the Lagrange multipliers for fulfilling the MP2 equations. The amplitudes z_i^a in $\hat{Z}$ ensure the Brillouin condition. If the frozen core approximation is used, the off-diagonal elements f_j^I must be fixed to zero, too (where I runs over frozen occupied orbitals and j over occupied orbitals that are included in the correlation treatment). The functional is stationary if all equations are fulfilled and it allows to directly eliminate the perturbation dependence of $\hat{T}_2$ and $\hat{R}$ from the expression for the density matrix.

To extend the Lagrange functional for the case of a solvated molecule, we replace in eq 83 E_0 by $E_{0,\mathrm{solv}}$, eq 38 and $\hat{F}_N$ by $\hat{F}_{N,\mathrm{solv}}$, eq 40. However, we do not include the additional term that originates from the creation of solvent charges; cf. section 2.1. This is because we want to define a purely molecular property. The derivative of the cavity contributions would add the properties of the polarizable external medium, which in our view is not a *molecular* property. To our knowledge this definition of molecular properties in condensed phase has always (tacitly) been assumed in the previous literature.

From the Lagrange functional, it follows that the ADC(2) one-particle excited state densities have three contributions: $P_q^p = \tilde{P}_q^p + X_q^p + Z_q^p$. The first one only includes the contributions from the excitation vectors:

$$\tilde{P}_j^i = -(R^\dagger)_i^c R_c^j - \frac{1}{2}(R^\dagger)_{il}^{cd} R_{cd}^{jl} \tag{84}$$

$$\tilde{P}_a^i = (R^\dagger)_k^c R_{ac}^{ik} \tag{85}$$

$$\tilde{P}_i^a = (R^\dagger)_{ik}^{ac} R_k^c \tag{86}$$

$$\tilde{P}_b^a = (R^\dagger)_k^a R_b^k + \frac{1}{2}(R^\dagger)_{kl}^{ad} R_{bd}^{kl} \tag{87}$$

The second contribution includes the MP2 amplitudes and the corresponding Lagrange multipliers

$$X_j^i = -\frac{1}{2} n_{jl}^{cd} t_{cd}^{il} \tag{88}$$

$$X_b^a = \frac{1}{2} n_{kl}^{ad} t_{bd}^{kl} \tag{89}$$

Actually, the expressions eqs 88 and 89 are not inherently symmetric. This comes from the asymmetric definition of the Lagrange functional but is inconsequential for expectation values of symmetric one-particle operators. For full consistency, one may symmetrize the Lagrangian [and consequently eqs 88 and 89]. The amplitudes n_{ij}^{ab} are obtained from

$$\langle 0|N_2 F_N a_{ij}^{ab}|0\rangle = -\langle 0|R_1^\dagger [H_N, a_{ij}^{ab}] R_1|0\rangle \tag{90}$$

which (for canonical orbitals) can be directly inverted, yielding a modified MP2-like expression for n_{ij}^{ab}.

Requiring stationarity of eq 83 with respect to orbital rotations, gives the Z-vector (or CPHF) equations,

$$Z_j^b \mathcal{A}_{ib}^{aj} = -\mathcal{Y}_i^a \tag{91}$$

where

$$\mathcal{A}_{ib}^{aj} = \delta_j^i f_b^a - \delta_b^a f_j^i + g_{i,b}^{a,j} - g_{b,i}^{a,j} - g_{a,b}^{i,j} \tag{92}$$

The right-hand side reads

$$\mathcal{Y}_q^p = f_c^p \bar{P}_q^c - f_k^p \bar{P}_q^k - \bar{P}_c^p f_q^c + \bar{P}_k^p f_q^k + g_{cs}^{pr} P_{qr}^{cs} - g_{ks}^{pr} P_{qr}^{ks} - P_{cs}^{pr} g_{qr}^{cs} + P_{ks}^{pr} g_{qr}^{ks} \tag{93}$$

with $\bar{P}_q^p = \tilde{P}_q^p + X_q^p$ and P_{qs}^{pr} as defined in Table 5.

Table 5. Definition of the Effective ADC(2) Two-Particle Density Needed in Equation 93[a]

$$P_{ab}^{ij} = t_{ab}^{ij} + \frac{1}{2}\hat{\mathcal{P}}_{ij}\hat{\mathcal{P}}_{ab}(R^\dagger)_k^c t_{ac}^{ik} R_b^j - \frac{1}{2}(R^\dagger)_k^c t_{ac}^{ij} R_b^k - \frac{1}{2}(R^\dagger)_k^c t_{ab}^{ik} R_c^j$$

$$P_{ij}^{ab} = n_{ij}^{ab} + \frac{1}{2}\hat{\mathcal{P}}_{ij}\hat{\mathcal{P}}_{ab}(R^\dagger)_i^a (t^\dagger)_{jk}^{bc} R_c^k - \frac{1}{2}(R^\dagger)_k^b (t^\dagger)_{ij}^{ac} R_c^k - \frac{1}{2}(R^\dagger)_j^c (t^\dagger)_{ik}^{ab} R_c^k$$

$$P_{ib}^{aj} = -(R^\dagger)_i^a R_b^j$$

$$P_{bc}^{ak} = \frac{1}{2}(R^\dagger)_l^a R_{bc}^{lk}$$

$$P_{jc}^{ik} = -\frac{1}{2}(R^\dagger)_j^d R_{dc}^{ik}$$

$$P_{ak}^{bc} = \frac{1}{2}(R^\dagger)_{lk}^{bc} R_a^l$$

$$P_{ik}^{dc} = -\frac{1}{2}(R^\dagger)_{ik}^{dc} R_d^j$$

[a]The operator $\hat{\mathcal{S}}_{pq}$ symmetrizes a matrix element according to $\hat{\mathcal{P}}_{pq} A_{rs}^{pq} = A_{rs}^{pq} - A_{rs}^{qp}$.

The contributions from the solvent are again present through the modified Fock operator. If the linear response terms, eqs 63 and 67, are included, some additional terms have to be added to the right-hand side. Using the intermediate $C_k^c = (t^\dagger)_{kl}^{cd} R_d^l$ these terms can be expressed as

$$\Delta\mathcal{Y}_i^a = (R^\dagger)_l^a B_{i,k}^{l,c} R_c^k - (R^\dagger)_i^d B_{d,k}^{a,c} R_c^k + \frac{1}{2}(R^\dagger)_l^a B_{i,c}^{l,k} C_k^c - \frac{1}{2}(R^\dagger)_i^d B_{d,c}^{a,k} C_k^c + \frac{1}{2}(C^\dagger)_a^l B_{l,k}^{i,c} R_c^k - \frac{1}{2}(C^\dagger)_d^i B_{a,k}^{d,c} R_c^k \tag{94}$$

and $\Delta\mathcal{Y}_a^i = -\Delta\mathcal{Y}_i^a$. The first two terms are also present for CIS; cf. ref 25.

■ ASSOCIATED CONTENT

Supporting Information

Cartesian coordinates of all discussed molecules, unless published previously; tables with the data used to generate the figures in this work. This material is available free of charge via the Internet at http://pubs.acs.org/.

■ AUTHOR INFORMATION

Corresponding Author

*E-mail: andreas.koehn@uni-mainz.de.

Notes

The authors declare no competing financial interest.

■ ACKNOWLEDGMENTS

This work was supported by the Deutsche Forschungsgemeinschaft (Heisenberg fellowship to A.K., KO 2337/3-1) and the Bundesministerium für Bildung und Forschung (cooperative project MESOMERIE, grant no. 13N10722). We thank Michael Diedenhofen (COSMOlogic, Leverkusen), Tobias

Schwabe (University of Hamburg), and Roberto Cammi (University of Parma) for useful comments on the manuscript.

REFERENCES

(1) Neugebauer, J.; Curutchet, C.; Munoz-Losa, A.; Mennucci, B. *J. Chem. Theory Comput.* **2010**, *6*, 1843.
(2) Lin, H.; Truhlar, D. G. *Theor. Chem. Acc.* **2007**, *117*, 185−199.
(3) Eichinger, M.; Tavan, P.; Hutter, J.; Parrinello, M. *J. Chem. Phys.* **1999**, *110*, 10452−10467.
(4) Olsen, J. M.; Aidas, K.; Kongsted, J. *J. Chem. Theory Comput.* **2010**, *6*, 3721−3734.
(5) Röhrig, U. F.; Frank, I.; Hutter, J.; Laio, A.; Vandevondele, J.; Rothlisberger, U. *ChemPhysChem* **2003**, *4*, 1177−1182.
(6) Sneskov, K.; Matito, E.; Kongsted, J.; Christiansen, O. *J. Chem. Theory Comput.* **2010**, *6*, 839−850.
(7) Sneskov, K.; Schwabe, T.; Kongsted, J.; Christiansen, O. *J. Chem. Phys.* **2011**, *134*, 104108.
(8) Schwabe, T.; Sneskov, K.; Olsen, J. M. H.; Kongsted, J.; Christiansen, O.; Hättig, C. *J. Chem. Theory Comput.* **2012**, DOI: 10.1021/ct3003749.
(9) Cramer, C. J.; Truhlar, D. G. *Chem. Rev.* **1999**, *99*, 2161−2200.
(10) Tomasi, J.; Mennucci, B.; Cammi, R. *Chem. Rev.* **2005**, *105*, 2999−3093.
(11) Tomasi, J. *WIREs Comput. Mol. Sci.* **2011**, *1*, 855−867.
(12) Klamt, A. *WIREs Comput. Mol. Sci.* **2011**, *1*, 699−709.
(13) Mennucci, B. *J. Phys. Chem. Lett.* **2010**, *1*, 1666.
(14) Miertus, S.; Scrocco, E.; Tomasi, J. *Chem. Phys.* **1981**, *55*, 117−129.
(15) Klamt, A.; Schüürmann, G. *J. Chem. Soc., Perkin Trans.* **1993**, *2*, 799−805.
(16) McRae, E. *J. Phys. Chem.* **1957**, *61*, 562−572.
(17) Kirkwood, J. G. *J. Chem. Phys.* **1934**, *2*, 351.
(18) Onsager, L. *J. Am. Chem. Soc.* **1936**, *58*, 1486−1493.
(19) Mikkelsen, K.; Ågren, H.; Jensen, H.-J. A.; Helgaker, T. *J. Chem. Phys.* **1988**, *89*, 3086.
(20) Mikkelsen, K.; Jørgensen, P.; Jensen, H.-J. A. *J. Chem. Phys.* **1994**, *100*, 6597.
(21) Mikkelsen, K.; Cesar, A.; Ågren, H.; Jensen, H.-J. A. *J. Chem. Phys.* **1995**, *103*, 9010.
(22) Christiansen, O.; Mikkelsen, K. *J. Chem. Phys.* **1999**, *110*, 8348.
(23) Cammi, R.; Mennucci, B. *J. Chem. Phys.* **1999**, *110*, 9877.
(24) Cammi, R.; Frediani, L.; Mennucci, B.; Ruud, K. *J. Chem. Phys.* **2003**, *119*, 5818.
(25) Cammi, R.; Mennucci, B.; Tomasi, J. *J. Phys. Chem. A* **2000**, *104*, 5631−5637.
(26) Caricato, M.; Mennucci, B.; Tomasi, J.; Ingrosso, F.; Cammi, R.; Corni, S.; Scalmani, G. *J. Chem. Phys.* **2006**, *124*, 124520.
(27) Mennucci, B.; Toniolo, A.; Cappelli, C. *J. Chem. Phys.* **1999**, *111*, 7197.
(28) Cammi, R. *J. Chem. Phys.* **2009**, *131*, 164104.
(29) Caricato, M.; Mennucci, B.; Scalmani, G.; Trucks, G. W.; Frisch, M. J. *J. Chem. Phys.* **2010**, *132*, 084102.
(30) Caricato, M. *J. Chem. Theory Comput.* **2012**, DOI: 10.1021/ct300382a.
(31) Cammi, R.; Fukuda, R.; Ehara, M.; Nakatsuji, H. *J. Chem. Phys.* **2010**, *133*, 024104.
(32) Müller, T.; Dallos, M.; Lischka, H.; Diedenhofen, M.; Klamt, A.; Monte, S. A. D. *Theor. Chem. Acc.* **2004**, *111*, 78−89.
(33) Schirmer, J. *Phys. Rev. A* **1982**, *26*, 2395−2416.
(34) Hättig, C. *Adv. Quantum Chem.* **2005**, *50*, 37−60.
(35) Christiansen, O.; Koch, H.; Jørgensen, P. *Chem. Phys. Lett.* **1995**, *243*, 409−418.
(36) Schreiber, M.; Silva, M. R. J.; Sauer, S. P. A.; Thiel, W. *J. Chem. Phys.* **2008**, *128*, 134110.
(37) Dreuw, A.; Weisman, J.; Head-Gordon, M. *J. Chem. Phys.* **2003**, *119*, 2943−2946.
(38) Plotner, J.; Tozer, D. J.; Dreuw, A. *J. Chem. Theory Comput.* **2010**, *6*, 2315−2324.
(39) Silva-Junior, M. R.; Schreiber, M.; Sauer, S. P. A.; Thiel, W. *J. Chem. Phys.* **2008**, *129*, 104103.
(40) Whitten, J. L. *J. Chem. Phys.* **1973**, *58*, 4496.
(41) Hättig, C.; Weigend, F. *J. Chem. Phys.* **2000**, *113*, 5154−5161.
(42) *TURBOMOLE* development version, 2011. For further information, see http://www.turbomole.com.
(43) Cammi, R.; Corni, S.; Mennucci, B.; Tomasi, J. *J. Chem. Phys.* **2005**, *122*, 104513.
(44) Corni, S.; Cammi, R.; Mennucci, B.; Tomasi, J. *J. Chem. Phys.* **2005**, *123*, 134512.
(45) Kongsted, J.; Osted, A.; Mikkelsen, K.; Christiansen, O. *Mol. Phys.* **2002**, *100*, 1813−1828.
(46) Olsen, J.; Jørgensen, P. In *Modern Electronic Structure Theory*; Yarkony, D. R., Ed.; World Scientific: Singapore, 1995; Vol. *2*; Chapter 13, pp 857−990.
(47) Mikkelsen, K.; Luo, Y.; Ågren, H.; Jørgensen, P. *J. Chem. Phys.* **1994**, *100*, 8240.
(48) Rösch, N.; Zerner, M. *J. Phys. Chem.* **1994**, *98*, 5817−5823.
(49) Iozzi, M.; Mennucci, B.; Tomasi, J.; Cammi, R. *J. Chem. Phys.* **2004**, *120*, 7029.
(50) Schäfer, A.; Klamt, A.; Sattel, D.; Lohrenz, J. C. W.; Eckert, F. *Phys. Chem. Chem. Phys.* **2000**, *2*, 2187−2193.
(51) Diedenhofen, M. In *High Performance Computing in Chemistry*; Grotendorst, J., Ed.; NIC Series; John von Neumann Institute for Computing: Jülich, 2005; Vol. *25*.
(52) Handy, N.; Schaefer, H. F., III *J. Chem. Phys.* **1984**, *81*, 5031.
(53) Head-Gordon, M.; Oumi, M.; Maurice, D. *Mol. Phys.* **1999**, *96*, 593−602.
(54) Head-Gordon, M.; Rico, R. J.; Oumi, M.; Lee, T. J. *Chem. Phys. Lett.* **1994**, *219*, 21−29.
(55) Schirmer, J.; Trofimov, A. *J. Chem. Phys.* **2004**, *120*, 11449−11464.
(56) Olivares del Valle, F. J.; Tomasi, J. *Chem. Phys.* **1991**, *150*, 139−150.
(57) Baldridge, K. K.; Jonas, V. *J. Chem. Phys.* **2000**, *113*, 7511.
(58) In the formulation of ref 55, the excited state density would also contain contributions from the second-order ground state wave function. This we want to avoid in our formulation. Although this approximation can be motivated by comparison to the structurally similar CC2 method, this definition may seem a bit arbitrary. The relaxed density, on the other hand, is strictly defined by gradient theory. Furthermore, as for the CC2 method, the orbital relaxed excited state properties are usually more accurate in our experience.
(59) Ángyán, J. G. *Chem. Phys. Lett.* **1995**, *241*, 51−56.
(60) Cammi, R.; Mennucci, B.; Tomasi, J. *J. Phys. Chem. A* **1999**, *103*, 9100−9108.
(61) Thouless, D. J. *Nucl. Phys.* **1961**, *22*, 78−95.
(62) Aidas, K.; Møgelhøj, A.; Nilsson, E. J. K.; Johnson, M. S.; Mikkelsen, K. V.; Christiansen, O.; Söderhjelm, P.; Kongsted, J. *J. Chem. Phys.* **2008**, *128*, 194503.
(63) The TURBOMOLE basis sets are available at ftp://ftp.chemie.uni-karlsruhe.de/pub/basen/.
(64) Helgaker, T.; Jørgensen, P.; Olsen, J. *Molecular Electronic-Structure Theory*; Wiley: New York, 2000.
(65) Klamt, A.; Jonas, V.; Bürger, T.; Lohrenz, J. C. W. *J. Phys. Chem. A* **1998**, *102*, 5074−5085.
(66) Foresman, J.; Keith, T.; Wiberg, K.; Snoonian, J.; Frisch, M. *J. Phys. Chem.* **1996**, *100*, 16098−16104.
(67) Davydov, A. S. *Theory of Molecular Excitons*; Plenum: New York, 1971.
(68) Förster, T. *Ann. Phys.* **1948**, *2*, 55−75.
(69) Hsu, C.; Fleming, G. R.; Head-Gordon, M.; Head-Gordon, T. *J. Chem. Phys.* **2001**, *114*, 3065.
(70) Liu, R.; Holman, M.; Zang, L.; Adams, D. *J. Phys. Chem. A* **2003**, *107*, 6522−6526.
(71) Köhn, A.; Hättig, C. *J. Am. Chem. Soc.* **2004**, *126*, 7399−7410.
(72) Grabowski, Z. R.; Rotkiewicz, K.; Siemiarczuk, A.; Cowley, D. J.; Baumann, W. *Nouv. J. Chim.* **1979**, *3*, 443−454.

(73) Grabowski, Z. R.; Rotkiewicz, K.; Rettig, W. *Chem. Rev.* **2003**, *103*, 3899−4032.
(74) Zachariasse, K.; Druzhinin, S.; Bosch, W.; Machinek, R. *J. Am. Chem. Soc.* **2004**, *126*, 1705−1715.
(75) Rappoport, D.; Furche, F. *J. Am. Chem. Soc.* **2004**, *126*, 1277−1284.
(76) Techert, S.; Zachariasse, K. *J. Am. Chem. Soc.* **2004**, *126*, 5593−5600.
(77) Hättig, C.; Hellweg, A.; Köhn, A. *J. Am. Chem. Soc.* **2006**, *128*, 15672−15682.
(78) Gómez, I.; Reguero, M.; Boggio-Pasqua, M.; Robb, M. *J. Am. Chem. Soc.* **2005**, *127*, 7119−7129.
(79) Lee, J.; Fujiwara, T.; Kofron, W.; Zgierski, M.; Lim, E. *J. Chem. Phys.* **2008**, *128*, 164512.
(80) Zachariasse, K.; Druzhinin, S.; Kovalenko, S.; Senyushkina, T. *J. Chem. Phys.* **2009**, *131*, 224313.
(81) Druzhinin, S.; Mayer, P.; Stalke, D.; von Bülow, R.; Noltemeyer, M.; Zachariasse, K. *J. Am. Chem. Soc.* **2010**, *132*, 7730−7744.
(82) Galván, I.; Martn, M.; Aguilar, M. *J. Chem. Theory Comput.* **2010**, *6*, 2445−2454.
(83) Coto, P. B.; Serrano-Andrés, L.; Gustavsson, T.; Fujiwara, T.; Lim, E. C. *Phys. Chem. Chem. Phys.* **2011**, *13*, 15182−15188.
(84) Rhinehart, J.; Challa, J.; McCamant, D. *J. Phys. Chem. B* **2012**, *116*, 10522−10534.
(85) Baumann, W.; Bischof, H.; Fröhling, J.-C.; Brittinger, C.; Rettig, W.; Rotkiewicz, K. *J. Photochem. Photobiol. A* **1992**, *64*, 49−72.